Design Guide: TIDA-010282

1.3kW GaN Totem Pole PFC and Motor Inverter Reference Design

Description

This reference design is a 1.3kW totem pole power factor correction (PFC) and motor inverter for major appliances and similar products. The design illustrates a method to implement digital totem pole PFC and sensorless vector control of three-phase permanent magnet synchronous motor (PMSM) to meet higher efficiency and low-profile requirements with a single C2000™ microcontroller. The hardware and software available with this reference design are tested and ready-to-use to accelerate development time to market.

Resources

TIDA-010282	Design Folder
TMS320F2800137, TMCS1126, LMG2650	Product Folder
LMG3651R025, TLV9062, LM2903B	Product Folder
UCC28881, UCC27712, TPS562206, TLV74033	Product Folder
C2000WARE-MOTORCONTROL-SDK	Tool Folder

Ask the TI E2E™ support experts

Features

- Wide operating voltage input range: 85V to 265 VAC, 50Hz and 60Hz
- Sensorless field-oriented control (FOC) motor control plus totem pole boost PFC converter control using a single C2000 controller
- Up to 1.3kW power output, 75kHz switching frequency, digital control totem pole boost PFC with power factor > 0.95 and < 5% THD from medium to full load over entire operating voltage range, robust adjustable voltage output with voltage and current fault protection
- Up to 1.3kW inverter stage, 15kHz switching frequency, torque compensation and automatic field weakening control for PMSM

Applications

- Air conditioner outdoor unit
- Refrigerator and freezer
- Washer and dryer
- Appliance: compressor

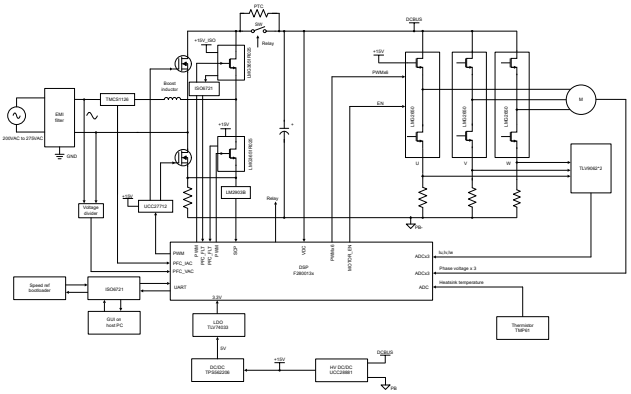

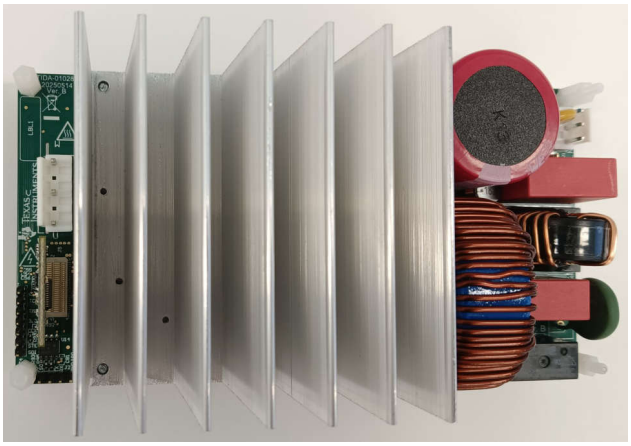

1 System Description

Modern major appliances demand high energy efficiency, small physical size, and lower costs while providing enhanced efficiency to consumers. Implementation of controlling a motor using sensorless field-oriented control (FOC) and digital totem pole PFC are illustrated. The overall Gallium Nitride (GaN) based system helps users to increase system efficiency, reduce board size, maximize power factor, precisely regulate the DC bus, and save development time. This reference design, based on the TMS320F280013x real-time controller family, provides a solid foundation for building robust control systems and accelerates development of advanced applications.

Totem pole PFC outperforms traditional boost PFC in terms of efficiency due to elimination of diode bridges and lower switching losses from high-performance GaN technology. GaN can also help to reduce boost inductor size by increasing switching frequency. Digitalized PFC enables straightforward regulation of DC bus voltage and effortless implementation of overvoltage, overtemperature, and overcurrent protection schemes.

The reference design integrates a dedicated, isolated, Universal Asynchronous Receiver-Transmitter (UART) port for direct debug access from a high-speed Graphical User Interface (GUI) on laptops.

1.1 Terminology

SLYZ022	TI Glossary: This glossary lists and explains terms, acronyms, and definitions
PMSM	Permanent Magnet Synchronous Motor
BLDC	Brushless Direct Current
BEMF	Back Electromotive Force
PWM	Pulse Width Modulation
MOSFET, FET	Metal Oxide Semiconductor Field Effect Transistor
IGBT	Insulated Gate Bipolar Transistor
RMS	Root Mean Square
MTPA	Maximum Torque Per Ampere
FWC	Field Weakening Control
PFC	Power Factor Correction
FOC	Field Oriented Control
HVAC	Heating, Ventilation, and Air Conditioning
ESMO	Enhanced Sliding-Mode Observer
PLL	Phase Locked Loop
FAST	Flux, Angle, Speed and Toque observer

1.2 Key System Specifications

Table 1-1. Key System Specifications

PARAMETERS	TEST CONDITIONS	MIN	NOM	MAX	UNIT
SYSTEM INPUT CHARACTERISTICS					
Input voltage (V_{INAC})	–	85	230	265	VAC
Input Frequency (f_{LINE})	–	47	50	63	Hz
No load standby power (P_{NL})	V_{INAC} = 230V, I_{out} = 0A	–	3.0	–	W
Input current (I_{IN})	V_{INAC} = 230V, I_{out} = I_{MAX}	–	5.65	6	A
PFC CONVERTER CHARACTERISTICS					
PWM switching frequency (f_{SW})	–	60	75	100	kHz
Output voltage (V_{OUT})	V_{IN} = nom, I_{OUT} = min to max	360	380	400	V
Output current (I_{OUT})	V_{IN} = min to max	–	–	4	A
Line regulation	V_{INAC} = min to max, I_{OUT} = nom	–	–	2	%
Load regulation	V_{INAC} = nom, I_{OUT} = min to max	–	–	3	%
Output voltage ripple	V_{INAC} = nom, I_{OUT} = max	–	–	20	V
Output over voltage	V_{INAC} = min to max	–	–	430	V

Table 1-1. Key System Specifications (continued)

PARAMETERS	TEST CONDITIONS	MIN	NOM	MAX	UNIT
DC-Link peak over current (I_{OCP})	V_{INAC} = min	–	–	8	A
Output power at high line	V_{INAC} = 250V	–	–	1.3	kW
Output power at low line	V_{INAC} = 187V	–	–	1.0	kW
Efficiency (Π)	V_{INAC} = nom at full load	–	99	–	%
MOTOR INVERTER CHARACTERISTICS					
PWM switching frequency (f_{SW})	–	–	15	–	kHz
Rated output power (P_{OUT})	V_{INAC} = nom	–	1.0	1.3	kW
Output current (I_{RMS})	V_{INAC} = nom	–	3.5	4.5	A
Inverter efficiency (Π)	V_{INAC} = nom, P_{OUT} = nom	–	99	–	%
Motor electrical frequency (f)	V_{INAC} = min to max	20	200	400	Hz
Fault protections	Overcurrent, stall, overtemperature, undervoltage, overvoltage				
Drive control method and features	Sensorless-FOC with three shunt resistors for current sensing				
SYSTEM CHARACTERISTICS					
Auxiliary power supply	V_{INAC} = min to max	15V±10%, 300mA			
Operating ambient	Open frame	–10	25	55	ºC
Standards and norms	Power line harmonics	EC 61000-3-2 Class A			
Board size	Length × width × height	150mm × 80mm × 55mm			mm^2

WARNING

TI intends this reference design to be operated in a lab environment only and does not consider the reference design to be a finished product for general consumer use.

TI Intends this reference design to be used only by qualified engineers and technicians familiar with risks associated with handling high-voltage electrical and mechanical components, systems, and subsystems.

High voltage! There are accessible high voltages present on the board. The board operates at voltages and currents that can cause shock, fire, or injury if not properly handled or applied. Use the equipment with necessary caution and appropriate safeguards to avoid injuring yourself or damaging property.

Hot surface! Contact can cause burns. **Do not touch!** Some components can reach high temperatures > 55°C when the board is powered on. The user must not touch the board at any point during operation or immediately after operating, as high temperatures can be present.

CAUTION

Do not leave the design powered when unattended.

2 System Overview

2.1 Block Diagram

Figure 2-1 shows the block diagram of this reference design with key TI components.

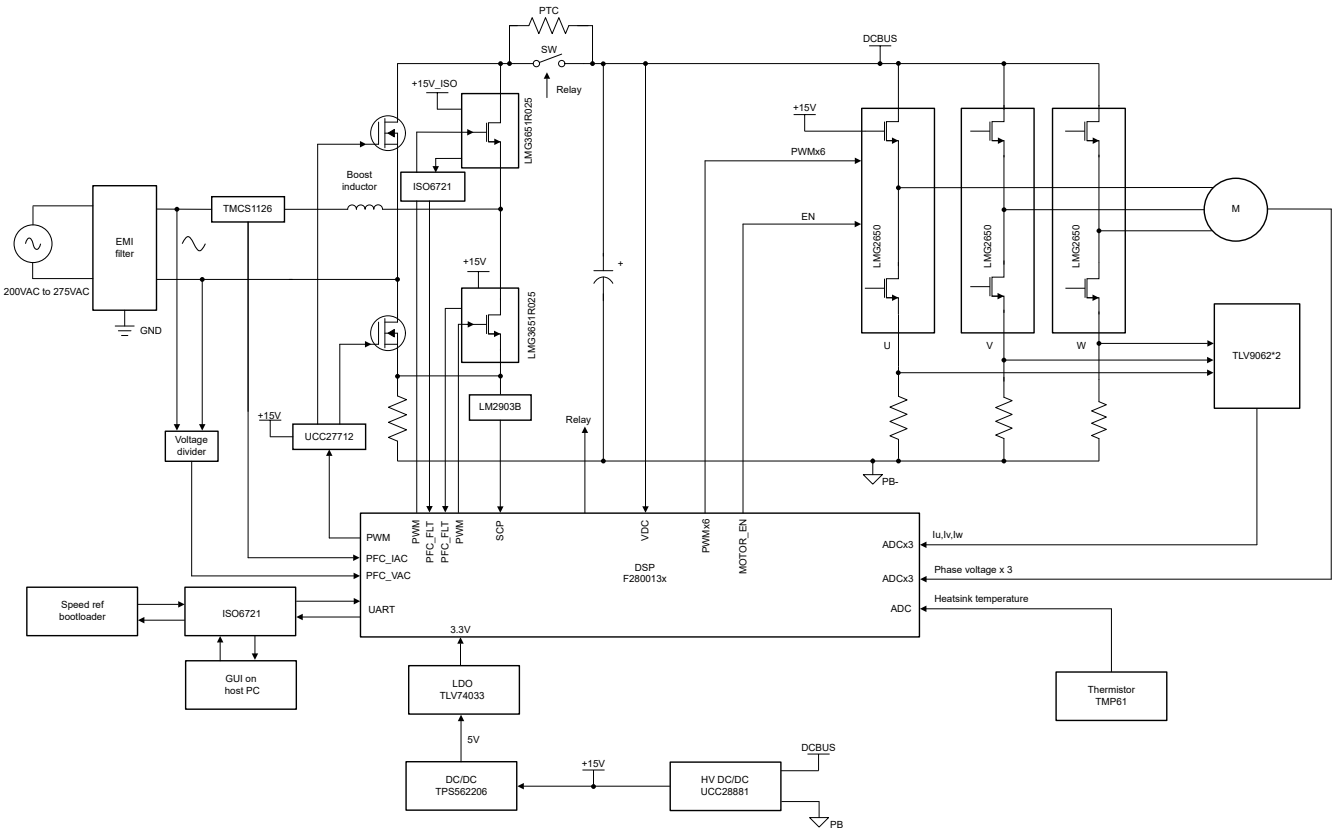

Figure 2-1. TIDA-010282 Totem Pole PFC and Motor Inverter Block Diagram

The entire system is represented in six blocks:

- Single-phase totem pole PFC
- Three-phase motor inverter
- Auxiliary power supply
- Isolated UART
- Microcontroller Unit
- Temperature sensing

2.2 Design Considerations

The design uses a single C2000 controller for both motor control and PFC. Highly noise-immune current and voltage sensing schemes are necessary for precise motor drive and PFC control. The following detail the sensing and drive circuit that are used on this design. The hardware design files are available under the C2000Ware Motor Control SDK Install directory at <install_location>\solutions\tida_010282_ttplpfcmc\hardware.

2.3 Highlighted Products

The following highlighted products are used in this reference design. Key features for selecting the devices for this reference design are revealed in this section. Find more details of the highlighted devices in the respective product data sheet.

2.3.1 TMS320F2800137

The TMS320F280013x is a member of the C2000™ real-time microcontroller family of scalable, ultra-low latency devices designed for efficiency in power electronics applications. The real-time control subsystem is based on TI's 32-bit C28x DSP core, which provides 120MHz of signal-processing performance for floating- or fixed-point code running from either on-chip flash or Static Random Access Memory (SRAM). The C28x Central Processing Unit (CPU)is further boosted by the Trigonometric Math Unit (TMU) and Cyclical Redundancy Check (VCRC) extended instruction sets, speeding up common algorithms key to real-time control systems. High-performance analog blocks are integrated on the F280013x real-time microcontroller (MCU) and are closely coupled with the processing and PWM units to provide excellent real-time signal chain performance. Fourteen PWM channels, all supporting frequency-independent resolution modes, enable control of various power stages from a three-phase inverter to advanced multilevel power topologies. Interfacing is supported through various industry-standard communication ports (such as Serial Peripheral Interface (SPI), three SCI, UART, I2C, and Controller Area Network (CAN)) and offers multiple pin-multiplexing options for excellent signal placement.

2.3.2 LMG3651R025

The LMG3651R025 GaN Field-Effect Transistor (FET) with integrated driver and protection is targeted at switch-mode power converters and enables designers to achieve new levels of power density and efficiency. Adjustable gate driver strength allow the control of turn-on and maximum turn-off slew rates independently, which can be used to actively control Electromagnetic Interference (EMI) and optimize switching performance. Turn on slew rate can be varied from 10V/ns to 100V/ns, while the turn-off slew rate can be limited from 10V/ns to a maximum based on the magnitude of load current. Protection features include undervoltage lockout (UVLO), cycle-by-cycle overcurrent limit, short-circuit and overtemperature protection. The LMG3651R025 provides a 5V low dropout (LDO) output on the LDO5V pin that can be used to power an external digital isolator.

2.3.3 LMG2650

The LMG2650 is a 650V, 95mΩ, GaN-powered, FET half bridge. The LMG2650 simplifies design, reduces component count, and reduces board space by integrating half-bridge power FETs, gate drivers, bootstrap diodes, and high-side gate-drive level shifters in a 6mm by 8mm QFN package. Programmable turn-on slew rates provide EMI and ringing control. The high-side gate-drive signal level shifter reliably transmits the INH pin signal to the high-side gate driver in challenging power switching environments. The smart-switched GaN bootstrap FET has no diode forward-voltage drop, avoids overcharging the high-side supply, and has zero reverse-recovery charge. The LMG2650 protection features include FET turn-on interlock, undervoltage lockout (UVLO), cycle-by-cycle current limit, and overtemperature shut down. The ultra-low slew rate setting supports motor drive applications.

2.3.4 TMCS1126

The TMCS1126 is a galvanically isolated Hall-effect current sensor with industry-leading isolation and accuracy. An output voltage proportional to the input current is provided with excellent linearity and low drift at all sensitivity options. Precision signal conditioning circuitry with built-in drift compensation is capable of less than 1.4% maximum sensitivity error over temperature and lifetime with no system-level calibration, or less than 0.9% maximum sensitivity error including both lifetime and temperature drift with a one-time calibration at room temperature.

Differential Hall-effect sensors reject interference from stray external magnetic fields. Insulation capable of withstanding $5kV_{RMS}$, coupled with a minimum of 8mm creepage and clearance, provides high levels of reliable lifetime reinforced working voltage. Integrated shielding enables excellent common-mode rejection and transient immunity. Fixed sensitivity allows the device to operate from a single 3V to 5.5V power supply, eliminating ratiometric errors and improving supply noise rejection.

2.3.5 ISO6721

The ISO6721 device is a high-performance, dual-channel digital isolator designed for cost-sensitive applications requiring up to 3000V_{RMS} (D package) isolation ratings per UL 1577. This device is also certified by VDE, TUV, CSA, and CQC. The ISO672xB devices provide high electromagnetic immunity and low emissions at low power consumption, while isolating Complementary Metal-Oxide-Semiconductor (CMOS) or Low-Voltage Complementary Metal-Oxide-Semiconductor (LVCMOS) digital I/Os. Each isolation channel has a logic input and output buffer separated by TI's double capacitive silicon dioxide (SiO2) insulation barrier. The ISO6720B device has two isolation channels with both channels in the same direction. The ISO6721B device has two isolation channels with 1 channel in each direction. Used in conjunction with isolated power supplies, these devices help prevent noise currents on data buses, such as UART, SPI, RS-485, RS-232, and CAN from damaging sensitive circuitry.

2.3.6 UCC28881

The UCC28881 integrates the controller and a 1Ω, 70V power MOSFET into one monolithic device. The device also integrates a high-voltage current source, enabling start-up and operation directly from the rectified mains voltage. The UCC28881 is the same family device of the UCC28880, with higher current. The low-quiescent current of the device enables excellent efficiency. With the UCC28881, the most common converter topologies, such as buck, buck boost, and flyback can be built using a minimum number of external components.

2.3.7 UCC27712

The UCC27712 is a 620V, high-side and low-side gate driver with 1.8A source, 2.8A sink current, targeted to drive power Metal-Oxide-Semiconductor Field-Effect Transistors (MOSFET) or Insulated Gate Bipolar Transistors (IGBT). The recommended VDD operating voltage is 10V to 20V for IGBTs and 10V to 17V for power MOSFETs. The UCC27712 includes protection features where the outputs are held low when the inputs are left open or when the minimum input pulse width specification is not met. Interlock and dead-time functions prevent both outputs from being turned on simultaneously.

2.3.8 TPS562206

The TPS562206 is a simple, easy-to-use, 2A synchronous buck converter in a SOT563 package. The device is designed to operate with minimum external component counts and also designed to achieve low standby current. This switch mode power supply (SMPS) device employs D-CAP3 control mode, providing a fast transient response and supporting both low-equivalent series resistance (ESR) output capacitors, such as specialty polymer and ultra-low ESR ceramic capacitors with no external compensation components. TPS562206 operates in FCCM mode, which keeps the same frequency and lower output ripple during all load conditions.

2.3.9 TLV9062

The TLV9062 is dual-low-voltage (1.8V to 5.5V) operational amplifier (op amp) with rail-to-rail input- and output-swing capabilities. These devices are highly cost-effective designs for applications where low-voltage operation, a small footprint, and high capacitive load drive are required. Although the capacitive load drive of the TLV906x is 100pF, the resistive open-loop output impedance simplifies stabilization with higher capacitive loads. The TLV906xS devices include a shutdown mode that allow the amplifiers to switch into standby mode with typical current consumption less than 1µA. The TLV906xS family helps simplify system design, because the family is unity-gain stable, integrates the RFI and EMI rejection filter, and provides no phase reversal in overdrive condition.

2.3.10 TLV74033

The TLV74033 low-dropout (LDO) linear regulator is a low quiescent current LDO with excellent line and load transient performance designed for power-sensitive applications. This device provides a typical accuracy of 1%. The TLV740P also provides inrush current control during device power up and enabling. The TLV740P limits the input current to the defined current limit to avoid large currents from flowing from the input power source. This functionality is especially important in battery-operated devices.

3 System Design Theory

The main focus of this reference design is totem pole PFC and motor control using sensorless-FOC with a low EMI, high efficiency, high power factor, and protected power rail for targeted major appliances and similar applications.

3.1 Totem Pole PFC

Boost converters dominate PFC applications due to continuous input current, which can be controlled using average current mode control. The converter forces input current to match phase changes in line voltage. High inherent efficiency and wide duty cycle range make boost converters more attractive.

While a basic single-phase boost converter is adequate for low-power, non-isolated applications, GaN totem pole PFC techniques provide additional advantages in high-power and highly efficient applications. Totem pole PFC increases efficiency since this removes the diode bridge, GaN furthermore reduces inductance size by increasing switching frequency since GaN has low switching loss.

3.1.1 Inductor Ratings

This section provides the procedures for calculating the inductor value and current rating.

- Value of Inductor

$$L_1 = \frac{\sqrt{2} \times V_{ACMIN} \times D_{MIN}}{\Delta I_L \times F_{SW}} \quad (1)$$

  ΔI_L is the peak-to-peak ripple current and most common design practices recommend limiting peak-to-peak ripple current at 20-25% of the average inductor current.

  – Peak-to-peak inductor current rating can be determined using Equation 2:

$$\Delta I_L = \%\ Ripple \times I_{L(AVG)} \quad (2)$$

  – Average inductor current can be determined using Equation 3:

$$I_{L(AVG)} = \frac{\sqrt{2} \times I_{LINE\_RMS\_MAX}}{2} \quad (3)$$

- Inductor Current Rating
  – Peak inductor current rating can be determined using Equation 4:

$$I_{L2_{PEAK}} = I_{L2_{PEAK}} = I_{L(AVG)} + \left(\frac{\Delta i_L}{2}\right) \quad (4)$$

3.1.2 AC Voltage Sensing

The AC voltage sensing circuit is used to convert the grid voltage signal into a low voltage signal, and then to condition these sensed signals to meet the requirements of the ADC input port. The line and the neutral voltages are sensed by the resistor divider to the reference point of the board as shown in Figure 3-1. The two signals are subtracted by the software to get the VAC sensing value.

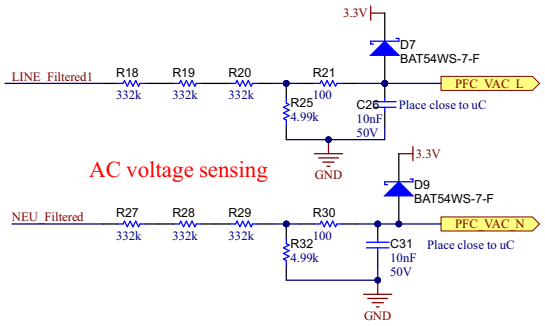

Figure 3-1. Input AC Voltage Sensing Circuit

3.1.3 DC Link Voltage Sensing

The DC bus voltage sensing circuit is used to convert the DC link voltage signal into a low voltage signal which is sensed by a resistor divider network as shown in Figure 3-2.

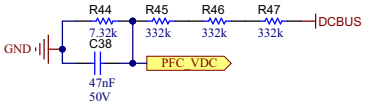

Figure 3-2. DC Bus Voltage Sensing Circuit

3.1.4 AC Current Sensing

The AC current sensing circuit is used to convert the PFC inductor current signal into a low voltage signal, and then to condition the sensed signal to meet the requirements of the ADC input port. As part of PFC inner current loop control, AC current sensing is crucial for both bandwidth and accuracy. A TMCS1126B4 is used for AC current sensing as shown in Figure 3-3.

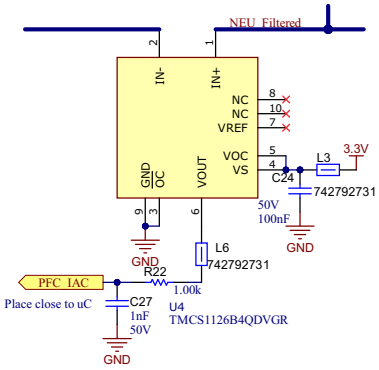

Figure 3-3. PFC AC Current Sensing Circuit

- AC current gain, the TMCS1126B4 has 100mV/A sensitivity.

$$V_{PFC\_IAC} = I_{AC\_PFC} \times G_i \tag{5}$$

$$V_{PFC\_IAC} = 0.1 \times I_{AC} \tag{6}$$

3.1.5 DC Link Capacitor Rating

The TIDA-010282 uses an aluminum electrolyte capacitor for the DC link. Although polymer electrolytic capacitors with the significantly longer lifetime have a proven high reliability, these capacitors are not the best choice because of a high-vibration environment like an outdoor compressor unit. Unlike liquid electrolytes in an aluminum electrolyte capacitor, polymer electrolyte capacitor cannot absorb vibration because of the solid polymer structure. To absorb a high-frequency component on DC link, a ceramic capacitor is also used in DC link close to the boost stage to reduce high-frequency loop.

- Capacitance Value Calculation
  - Value of DC link capacitor based on holdup charge

$$C_{OUT(MIN)} \geq \frac{2 \times P_{OUT} \times \frac{1}{f_{LINE}}}{V_{OUT}^2 - \left(\frac{V_{OUT}}{2}\right)^2} \tag{7}$$

  - Value of DC link capacitor value based upon voltage ripple requirement

$$C_{OUT(MIN)} = \frac{1}{4} \times \frac{\left(\frac{P_{OUT}}{V_{OUT} \times \eta \times 0.637}\right)}{V_{RIPPLE} \times 0.8 \times \pi \times f_{LINE}} \tag{8}$$

  - Capacitor Derating

Actual capacitor value changes based upon factors like initial capacitor tolerance, temperature and aging. Consider 20% for each factor.

$$C_{OUT} = \frac{C_{OUT(MIN)}}{\left(1-\eta_{tolerance}\right)\times\left(1-\eta_{temp}\right)\times\left(1-\eta_{aging}\right)} \quad (9)$$

- Capacitance Voltage Rating
  - Considering peak ripple voltage

$$WV_{DC\_BUS\_CAP\_MIN} = V_{DCBUS} + \frac{\Delta V_{PP}}{2} \quad (10)$$

  - Considering 10% safety margin for transient and overvoltage

$$WV_{DC\_BUS\_CAP} = 1.1 \times WV_{DC\_BUS\_CAP\_MIN} \quad (11)$$

- Capacitance Current RMS Value

  Estimating the capacitor RMS current is not straightforward and needs following steps:

  - Angular frequency is given by

$$\omega = 2 \times \pi \times f_{LINE} \quad (12)$$

  - Number of iterations

$$iteration = \frac{F_{SW\_PFC}}{2 \times F_{LINE}} \quad (13)$$

  - Value of one step in seconds:

$$Step = \frac{\frac{1}{f_{LINE}}}{Iteration} \quad (14)$$

  - Line voltage is a sine function and can be determined with

$$V_{IN}(t) = \sqrt{2} \times V_{IN(RMS)} \times \sin(\omega t) \quad (15)$$

  - Duty Ratio is also function of input voltage and can be calculated as

$$D(t) = \frac{V_{OUT} - V_{IN}(\omega t)}{V_{OUT}} \quad (16)$$

  - With power factor correction, input current is also sine function

$$I_{IN}(t) = \frac{\sqrt{2} \times P_{OUT}}{\eta_{System} \times V_{IN(MIN)}} \times \sin(\omega t) \quad (17)$$

$$I_{Crms} = \sqrt{\frac{1}{Iteration} \times \sum_{n=1}^{Iteration} \left\{ [I_{IN}(n \times Step)]^2 \times \left[\frac{1}{2} \times \sqrt{(2 - 2 \times D(n \times Step)) - (2 - 2 \times D(n \times Step))^2} \right]^2 \right\}} \quad (18)$$

- Capacitor ESR Rating

$$ESR_{MAX} \geq \frac{V_{RIPPLE} \times 0.2}{\left(\frac{P_{OUT} \times \sqrt{2}}{V_{IN(MIN)} \times \eta}\right)} \quad (19)$$

3.2 Three-Phase PMSM Drive

Permanent Magnet Synchronous motor (PMSM) has a wound stator, a permanent magnet rotor assembly and internal or external devices to sense rotor position. The sensing devices provide position feedback for adjusting frequency and amplitude of stator voltage reference properly to maintain rotation of the magnet assembly. The combination of an inner permanent magnet rotor and outer windings offers the advantages of low rotor inertia, efficient heat dissipation, and reduction of the motor size.

- Synchronous motor construction: Permanent magnets are rigidly fixed to the rotating axis to create a constant rotor flux. This rotor flux typically has a constant magnitude. The stator windings, when energized, create a rotating electromagnetic field. To control the rotating magnetic field, this is necessary to control the stator currents.
- The actual structure of the rotor varies depending on the power range and rated speed of the machine. Permanent magnets are designed for synchronous machines ranging up-to a few kilowatts. For higher power ratings, the rotor typically consists of windings in which a DC current circulates. The mechanical structure of the rotor is designed for the number of poles desired, and the desired flux gradients desired.
- The interaction between the stator and rotor fluxes produces a torque. Since the stator is firmly mounted to the frame, and the rotor is free to rotate, the rotor can rotate, producing a useful mechanical output as shown in Figure 3-4.
- The angle between the rotor magnetic field and stator field must be carefully controlled to produce maximum torque and achieve high electromechanical conversion efficiency. For this purpose a fine tuning is needed after closing the speed loop using a sensorless algorithm to draw the minimum amount of current under the same speed and torque conditions.
- The rotating stator field must rotate at the same frequency as the rotor permanent magnetic field; otherwise, the rotor can experience rapidly alternating positive and negative torque. This can result in less-than-designed-for torque production, and excessive mechanical vibration, noise, and mechanical stresses on the machine parts. In addition, if the rotor inertia prevents the rotor from being able to respond to these oscillations, the rotor can stop rotating at the synchronous frequency, and respond to the average torque as seen by the stationary rotor: Zero. This means that the machine experiences a phenomenon known as *pull-out*. This is also the reason why the synchronous machine is not self starting.
- The angle between the rotor field and the stator field must be equal to 90º to obtain the highest mutual torque production. This synchronization requires knowing the rotor position to generate the right stator field.
- The stator magnetic field can be made to have any direction and magnitude by combining the contribution of different stator phases to produce the resulting stator flux.

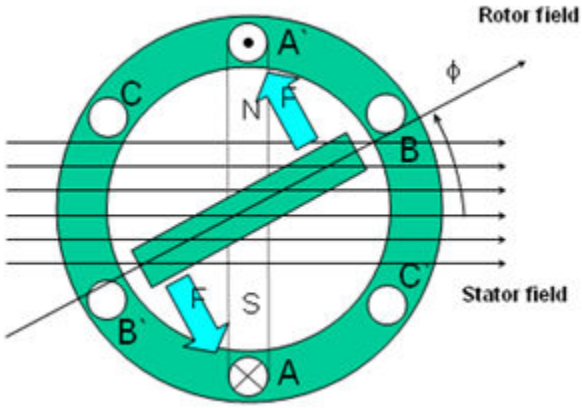

Figure 3-4. Interaction Between the Rotating Stator Flux, and the Rotor Flux Produces a Torque

3.2.1 Field Oriented Control of PM Synchronous Motor

To achieve better dynamic performance, a more complex control scheme needs to be applied, to control the PM motor. With the mathematical processing power offered by the microcontrollers, advanced control strategies can be implemented, which use mathematical transformations to decouple the torque generation and the magnetization functions in PM motors. Such de-coupled torque and magnetization control is commonly called rotor flux oriented control, or simply Field Oriented Control (FOC).

In a direct current (DC) Motor, the excitation for the stator and rotor is independently controlled, the produced torque and the flux can be independently tuned as shown in Figure 3-5. The strength of the field excitation (for example, the magnitude of the field excitation current) sets the value of the flux. The current through the rotor windings determines how much torque is produced. The commutator on the rotor plays an interesting part in the torque production. The commutator maintains contact with the brushes, and mechanical design

switches windings into the circuit that produce maximum torque when aligned. Mechanical construction manages windings that keep flux from rotor windings perpendicular to stator field at all times.

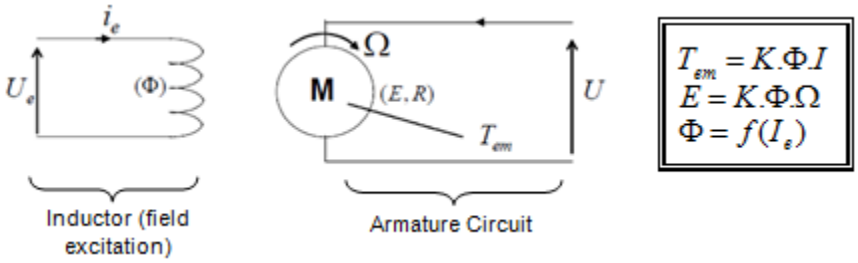

Figure 3-5. Flux and Torque are Independently Controlled in DC Motor Model

The goal of the FOC (also called vector control) on synchronous and asynchronous machines is to be able to separately control the torque producing and magnetizing flux components. FOC control allow us to decouple the torque and the magnetizing flux components of stator current. With decoupled control of the magnetization, the torque producing component of the stator flux can now be thought of as independent torque control. Decoupling the torque and flux is necessary to engage several mathematical transforms, and this is where the microcontrollers add the most value. The processing capability provided by the microcontrollers enables these mathematical transformations to be carried out very quickly. This, in turn, implies that the entire algorithm controlling the motor can be executed at a fast rate, enabling higher dynamic performance. In addition to the decoupling, a dynamic model of the motor is now used for the computation of many quantities such as rotor flux angle and rotor speed. This means that the effect is accounted for, and the overall quality of control is better.

According to the electromagnetic laws, the torque produced in the synchronous machine is equal to vector cross product of the two existing magnetic fields as Equation 20 shows.

$$\tau_{em} = \vec{B}_{stator} \times \vec{B}_{rotor} \tag{20}$$

This expression shows that the torque is maximum if stator and rotor magnetic fields are orthogonal meaning, if the load is maintained at 90 degrees. If this condition is maintained all of the time and if the flux is oriented correctly, reduce the torque ripple and provide a better dynamic response. However, the constraint is to know the rotor position: this can be achieved with a position sensor such as incremental encoder. For low-cost applications where the rotor is not accessible, different rotor position observer strategies are applied to get rid of the position sensor.

In brief, the goal is to maintain the rotor and stator flux in quadrature: the goal is to align the stator flux with the q axis of the rotor flux, for example, orthogonal to the rotor flux. To do this, the stator current component in quadrature with the rotor flux is controlled to generate the commanded torque, and the direct component is set to zero. The direct component of the stator current can be used in some cases for field weakening, which has the effect of opposing the rotor flux, and reducing the back-EMF, which allows for operation at higher speeds.

The Field Orientated Control consists of controlling the stator currents represented by a vector. This control is based on projections which transform a three phase time and speed dependent system into a two coordinate (d and q coordinates) time invariant system. These projections lead to a structure similar to that of a DC machine control. Field-orientated-controlled machines need two constants as input references: the torque component (aligned with the q coordinate) and the flux component (aligned with d coordinate). Because Field Orientated Control is simply based on projections, the control structure handles instantaneous electrical quantities. This makes the control accurate in every working operation (steady state and transient) and independent of the limited bandwidth mathematical model. The FOC thus solves the classic scheme problems, in the following ways:

- The ease of reaching constant reference (torque component and flux component of the stator current)
- The ease of applying direct torque control because in the (d, q) reference frame the expression of the torque is defined in Equation 21.

$$\tau_{em} \propto \psi_R \times i_{sq} \tag{21}$$

By maintaining the amplitude of the rotor flux (ψ_R) at a fixed value, a linear relationship between torque and torque component (i_{Sq}) if formed. Controlling the torque component of the stator current vector then controls the torque output.

3.2.1.1 Space Vector Definition and Projection

The three-phase voltages, currents, and fluxes of AC motors can be analyzed in terms of complex space vectors. With regard to the currents, the space vector can be defined as follows:

- Assuming that i_a, i_b, and i_c are the instantaneous currents in the stator phases, then the complex stator current vector is defined in Equation 22.

$$\bar{i}_s = i_a + \alpha i_b + \alpha^2 i_c \tag{22}$$

where

$\alpha = e^{j\frac{2}{3}\pi}$ and $\alpha^2 = e^{j\frac{4}{3}\pi}$ represent the spatial operators

Figure 3-6 shows the stator current complex space vector.

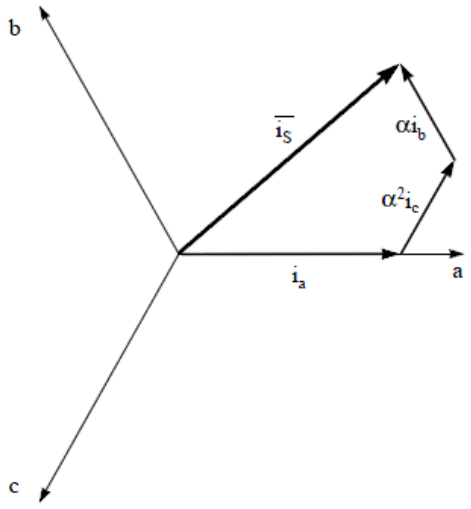

Figure 3-6. Stator Current Space Vector and Component in (a, b, c) Frame

In Figure 3-6, (a, b, and c) are the three-phase system axes. This current space vector depicts the three-phase sinusoidal system. This still needs to be transformed into a two-time invariant coordinate system. This transformation can be split into two steps:

$$(a,\ b) \Rightarrow (\alpha, \beta) \tag{23}$$

(Clarke transformation) which outputs a 2-coordinate time-variant system

$$(\alpha, \beta) \Rightarrow (d,\ q) \tag{24}$$

(Park transformation) which outputs a 2-coordinate time-invariant system

3.2.1.2 Clarke Transformation

The space vector can be reported in another reference frame with only two orthogonal axis called (α, β). Figure 3-7 shows the resulting vector diagram when assuming that the axis a and the axis alpha are in the same direction.

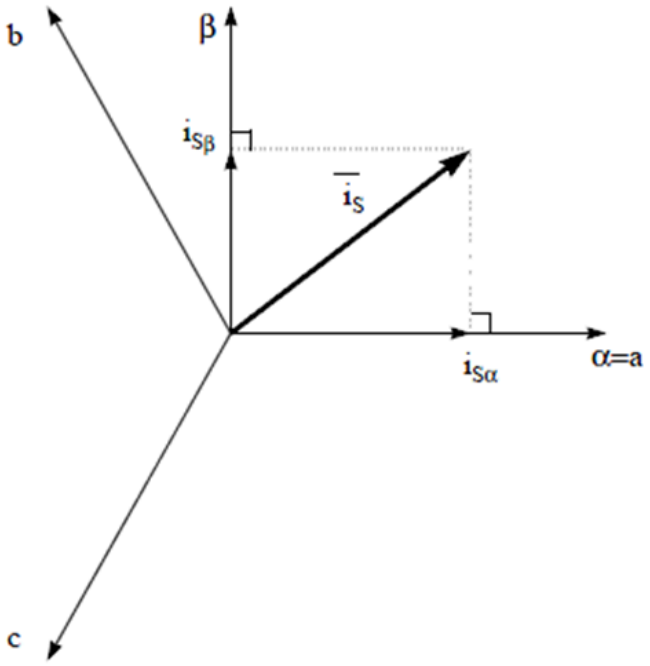

Figure 3-7. Stator Current Space Vector in the Stationary Reference Frame

Equation 25 shows the projection that modifies the three-phase system into the (α, β) 2-dimension orthogonal system.

$$i_{s\alpha} = i_a$$
$$i_{s\beta} = \frac{1}{\sqrt{3}} i_a + \frac{2}{\sqrt{3}} i_b \quad (25)$$

The two phase (α, β) currents are still depends on time and speed.

3.2.1.3 Park Transformation

The next step in system design is to modify a 2-phase orthogonal system (α, β) in the (d, q) rotating reference frame. Consider the d axis aligned with the rotor flux, Figure 3-8 shows the relationship for the current vector from the two-reference frame.

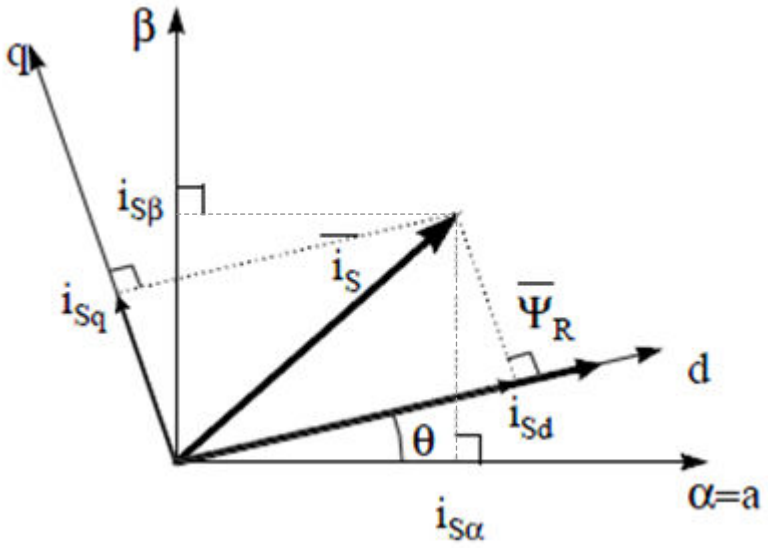

Figure 3-8. Stator Current Space Vector in the d,q Rotating Reference Frame

The flux and torque components of the current vector are determined by Equation 26.

$$i_{sd} = i_{s\alpha}\cos(\theta) + i_{s\beta}\sin(\theta)$$
$$i_{sq} = -i_{s\alpha}\sin(\theta) + i_{s\beta}\cos(\theta) \quad (26)$$

where

- θ is the rotor flux position

These components depend on the current vector (α, β) components and on the rotor flux position; if the right rotor flux position is known, then, by this projection the d,q component becomes a constant. Two phase currents now turn into dc quantity (time-invariant). At this point the torque control becomes easier where the constant i_{sd} (flux component) and the i_{sq} (torque component) current components are controlled independently.

3.2.1.4 Basic Scheme of FOC for AC Motor

Figure 3-9 summarizes the basic scheme of torque control with FOC.

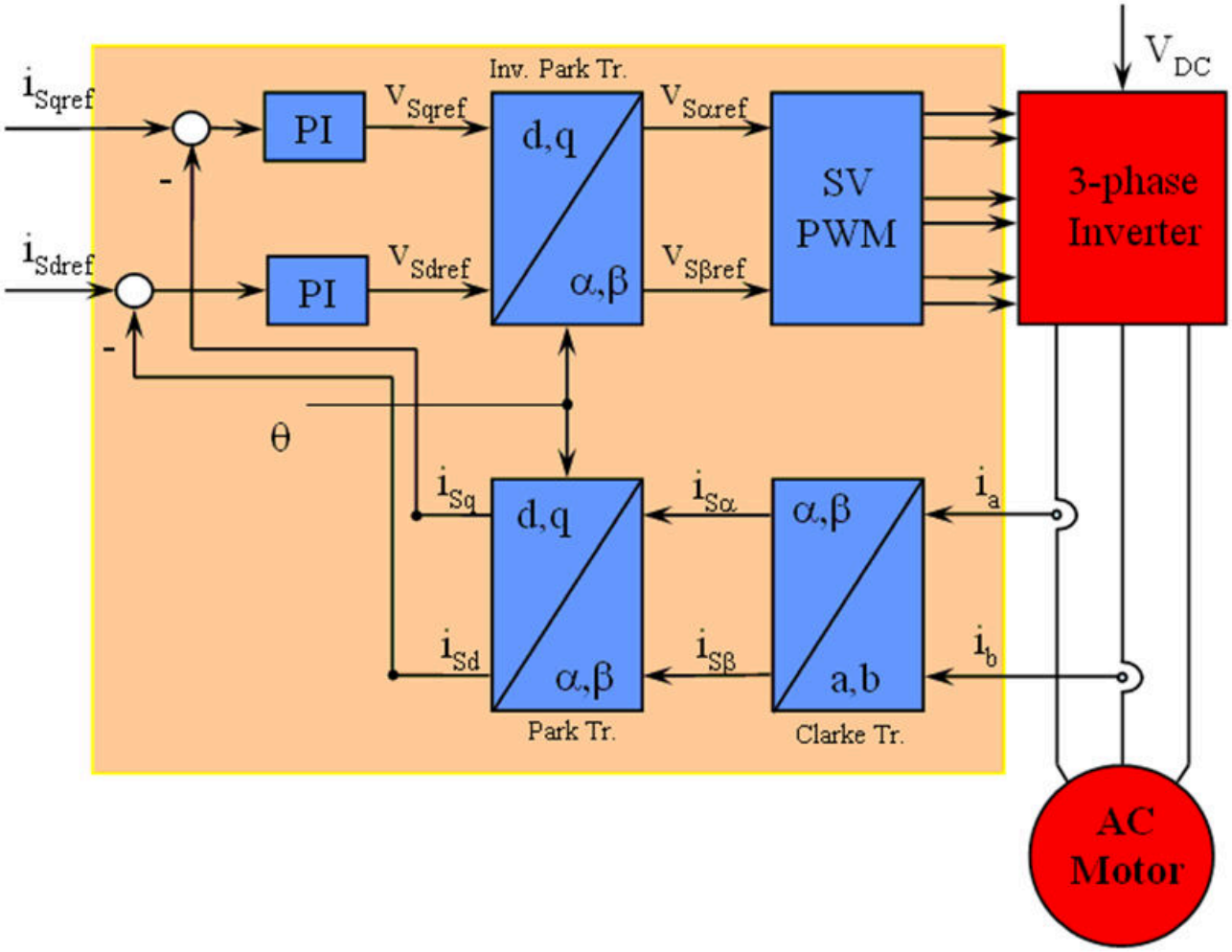

Figure 3-9. Basic Scheme of FOC for AC Motor

Two motor phase currents are measured. These measurements feed the Clarke transformation module. The outputs of this projection are designated $i_{s\alpha}$ and $i_{s\beta}$. These two components of the current are the inputs of the Park transformation that gives the current in the d,q rotating reference frame. The i_{sd} and i_{sq} components are compared to the references i_{sdref} (the flux reference component) and i_{sqref} (the torque reference component). At this point, this control structure shows an interesting advantage: this can be used to control either synchronous or induction machines by simply changing the flux reference and obtaining rotor flux position. As in a

synchronous permanent magnet, a motor, the rotor flux is fixed determined by the magnets; there is no need to create one. Hence, when controlling a PMSM, i_{sdref} needs to be set to zero. As an AC induction motor needs a rotor flux creation to operate, the flux reference must not be zero. This conveniently solves one of the major drawbacks of the *classic* control structures: the portability from asynchronous to synchronous drives. The torque command i_{sqref} can be the output of the speed regulator when using a speed FOC. The outputs of the current regulators are V_{sdref} and V_{sqref}; outputs are applied to the inverse Park transformation. The outputs of this projection are $V_{s\alpha ref}$ and $V_{s\beta ref}$ which are the components of the stator vector voltage in the (α, β) stationary orthogonal reference frame. These are the inputs of the Space Vector PWM. The outputs of this block are the signals that drive the inverter. Both the Park and inverse Park transformations need the rotor flux position. Obtaining this rotor flux position depends on the AC machine type (synchronous or asynchronous machine).

3.2.1.5 Rotor Flux Position

Knowledge of the rotor flux position is the core of the FOC. In fact if there is an error in this variable the rotor flux is not aligned with the d-axis and i_{sd} and i_{sq} are incorrect flux and torque components of the stator current. Figure 3-10 shows the (a, b, c), (α, β) and (*d, q*) reference frames, and the correct position of the rotor flux, the stator current and stator voltage space vector that rotates with d,q reference at synchronous speed.

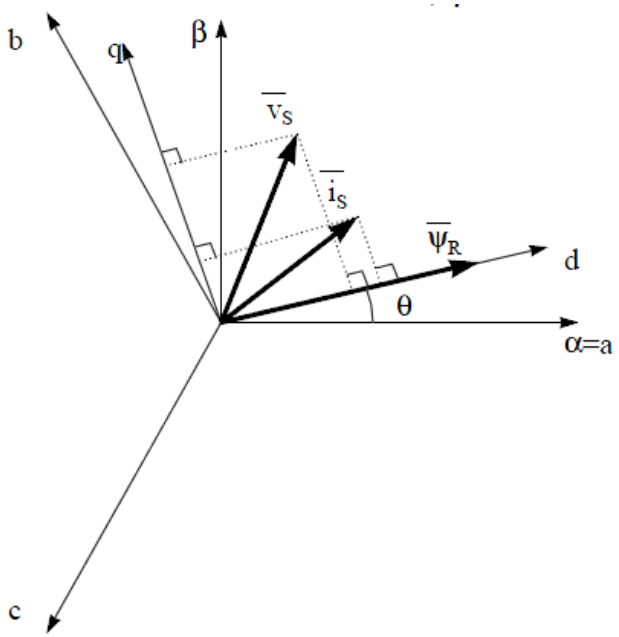

Figure 3-10. Current, Voltage and Rotor Flux Space Vectors in the (d, q) Rotating Reference Frame

The measure of the rotor flux position is different when considering the synchronous or asynchronous motor:

- In the synchronous machine the rotor speed is equal to the rotor flux speed. Then θ (rotor flux position) is directly measured by the position sensor or by integration of rotor speed.
- In the asynchronous machine the rotor speed is not equal to the rotor flux speed (there is a slip speed), then this needs a particular method to calculate θ. The basic method is the use of the current model which needs two equations of the motor model in the *d, q* reference frame.

Theoretically, the FOC for the PMSM drive allows the motor torque be controlled independently with the flux like DC motor operation. In other words, the torque and flux are decoupled from each other. The rotor position is required for variable transformation from the stationary reference frame to the synchronously rotating reference frame. As a result of this transformation (so called Park transformation), q-axis current can be controlling torque while d-axis current is forced to zero. Therefore, the key module of this system is the estimation of rotor position using enhance Sliding-Mode Observer (eSMO) or FAST estimator.

Figure 3-11 shows the overall block diagram of sensorless FOC of fan PMSM using eSMO with flying start.

Figure 3-12 shows the overall block diagram of sensorless FOC of compressor PMSM using eSMO with field weakening control (FWC) and maximum torque per ampere (MTPA) .

Figure 3-13 shows the overall block diagram of sensorless FOC of fan PMSM using FAST with flying start.

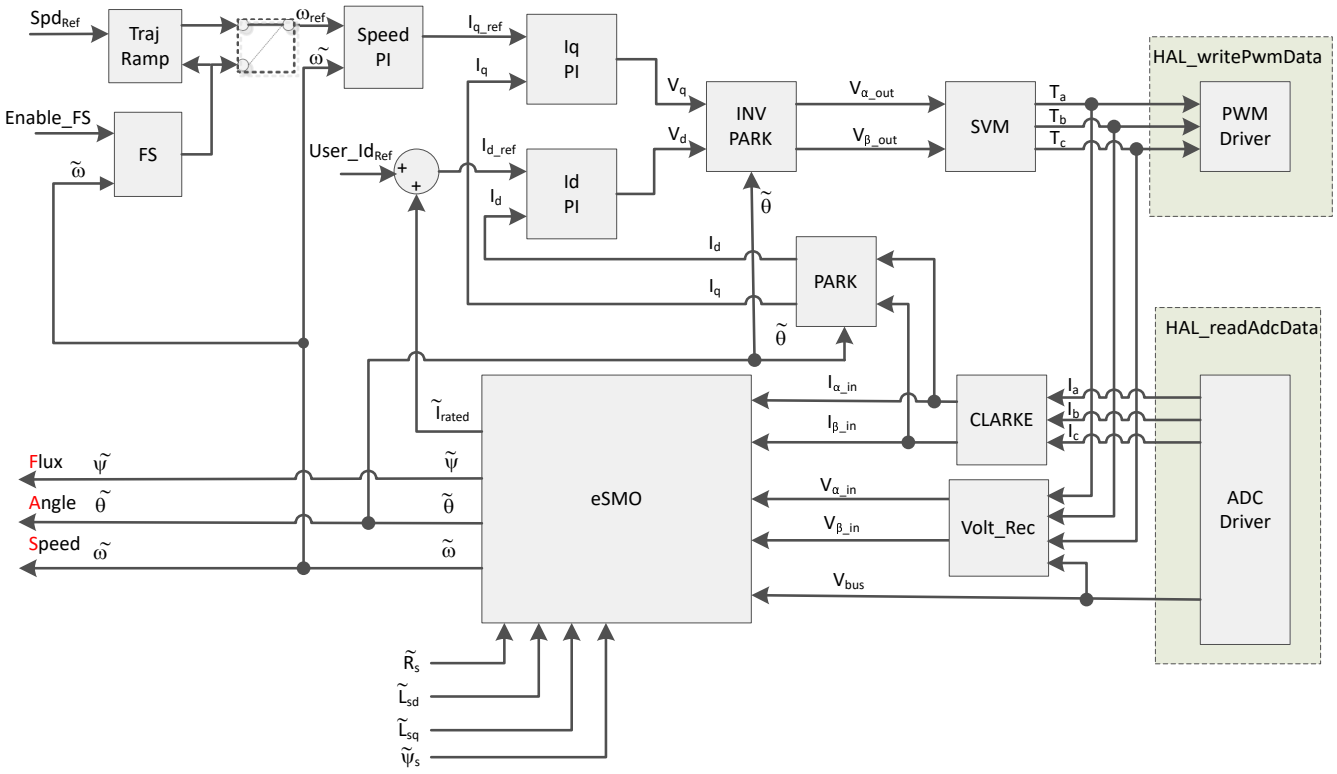

Figure 3-11. Sensorless FOC of Fan PMSM Using eSMO With Flying Start (FS)

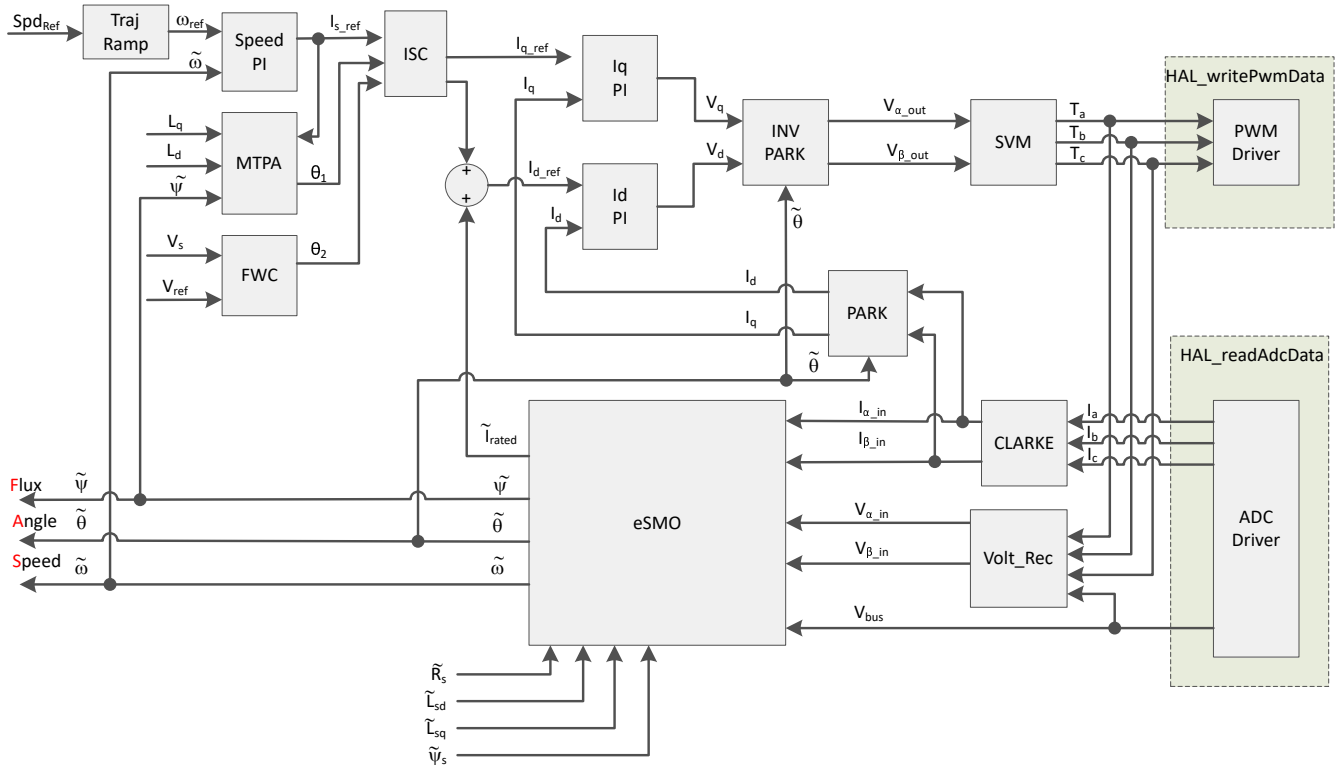

Figure 3-12. Sensorless FOC of compressor PMSM Using eSMO With FWC and MTPA

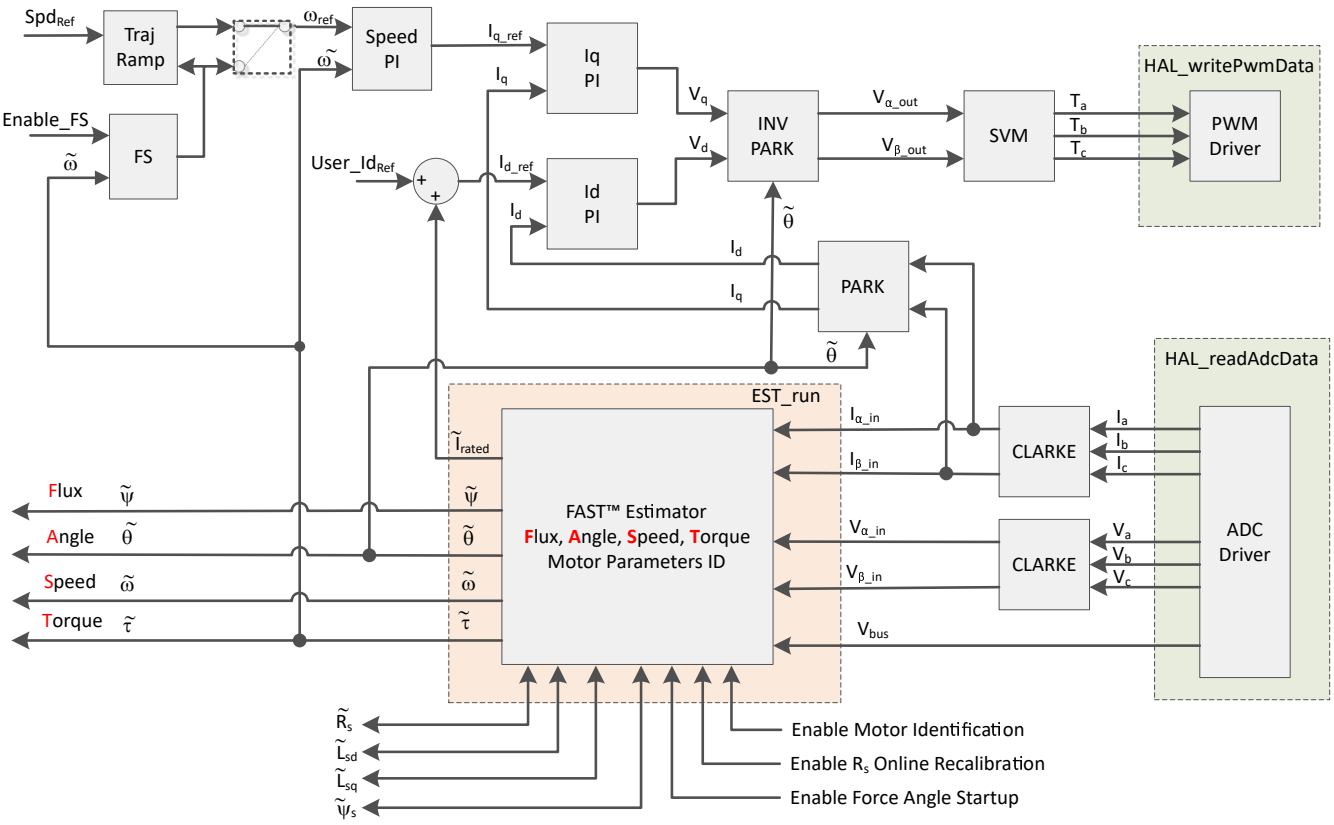

Figure 3-13. Sensorless FOC of Fan PMSM using FAST with Flying Start (FS)

3.2.2 Sensorless Control of PM Synchronous Motor

In home appliance applications, if the mechanical sensor is used, this can increase cost, size, and reliability problems. To overcome these problems, sensorless control methods are implemented. Several estimation methods exist to get the rotor speed and position information without mechanical position sensors. The sliding mode observer (SMO) is commonly used due to various attractive features including reliability, desired performance, and robustness against system parameter variations.

3.2.2.1 Enhanced Sliding Mode Observer With Phase Locked Loop

The model-based method is used to achieve position sensorless control of the IPMSM drive system when the motor runs at middle or high speed. The model method estimates the rotor position by the back-EMF or the flux linkage model. The sliding mode observer is an observer-design method based on sliding mode control. The structure of the system is not fixed but purposefully changed according to the current state of the system, forcing the system to move according to the predetermined sliding mode trajectory. The advantages include fast response, strong robustness, and insensitivity to both parameter changes and disturbances.

3.2.2.1.1 Mathematical Model and FOC Structure of an IPMSM

Figure 3-14 shows the sensorless FOC structure for an IPMSM. In this system, the eSMO is used for achieving the sensorless control of an IPMSM system, and the eSMO model is designed by utilizing the back-EMF model together with a PLL model for estimating the rotor position and speed.

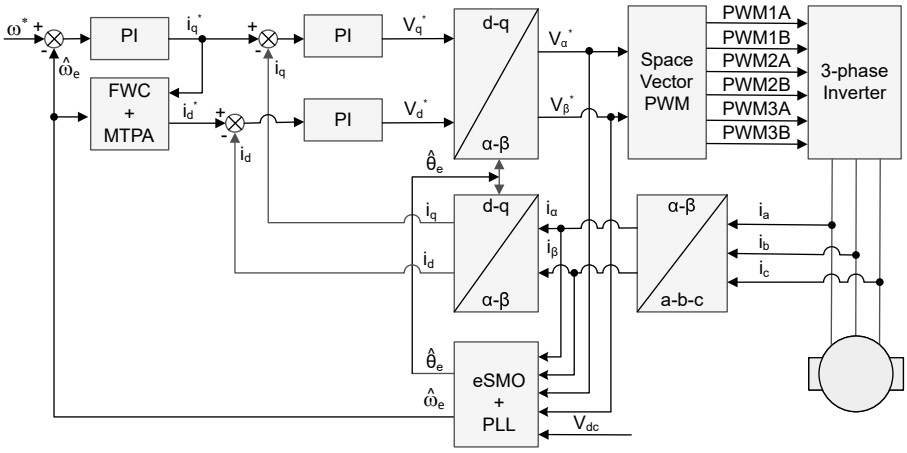

Figure 3-14. Sensorless FOC Structure of an IPMSM System

An IPMSM consists of a three-phase stator winding (a, b, c axes), and permanent magnets (PM) rotor for excitation. The motor is controlled by a standard three-phase inverter. An IPMSM can be modeled by using phase a-b-c quantities. Through proper coordinate transformations, the dynamic PMSM models in the d-q rotor reference frame and the α-β stationary reference frame can be obtained. The relationship among these reference frames are illustrated in Equation 27. The dynamic model of a generic PMSM can be written in the d-q rotor reference frame as:

$$\begin{bmatrix} v_d \\ v_q \end{bmatrix} = \begin{bmatrix} R_s + pL_d & -\omega_e L_q \\ \omega_e L_d & R_s + pL_q \end{bmatrix} \begin{bmatrix} i_d \\ i_q \end{bmatrix} + \begin{bmatrix} 0 \\ \omega_e \lambda_{pm} \end{bmatrix} \tag{27}$$

where

- v_d and v_q are the q-axis and d-axis stator terminal voltages, respectively
- i_d and i_q are the d-axis and q-axis stator currents, respectively
- L_d and L_q are the q-axis and d-axis inductances, respectively
- p is the derivative operator, a short notation of d/d_t
- λ_{pm} is the flux linkage generated by the permanent magnets
- R_s is the resistance of the stator windings
- ω_e is the electrical angular velocity of the rotor

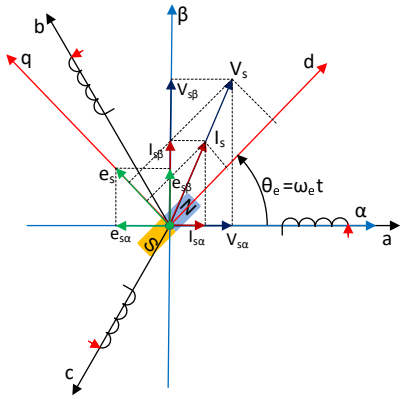

Figure 3-15. Definitions of Coordinate Reference Frames for PMSM Modeling

By using the inverse Park transformation as shown in Figure 3-15, the dynamics of the PMSM can be modeled in the α-β stationary reference frame as:

$$\begin{bmatrix} v_\alpha \\ v_\beta \end{bmatrix} = \begin{bmatrix} R_s + pL_d & \omega_e\left(L_d - L_q\right) \\ -\omega_e\left(L_d - L_q\right) & R_s + pL_q \end{bmatrix} \begin{bmatrix} i_\alpha \\ i_\beta \end{bmatrix} + \begin{bmatrix} e_\alpha \\ e_\beta \end{bmatrix} \tag{28}$$

where

- e_α and e_β are components of extended electromotive force (EEMF) in the α-β axis and can be defined as Equation 29 shows.

$$\begin{bmatrix} e_\alpha \\ e_\beta \end{bmatrix} = \left(\lambda_{pm} + \left(L_d - L_q\right) i_d\right) \omega_e \begin{bmatrix} -\sin(\theta_e) \\ \cos(\theta_e) \end{bmatrix} \tag{29}$$

According to Equation 28 and Equation 29, the rotor position information can be decoupled from the inductance matrix by means of the equivalent transformation and the introduction of the EEMF concept, so that the EEMF is the only term that contains the rotor pole position information. Now the EEMF phase information can be directly used to realize the rotor position observation. Rewrite the IPMSM voltage equation Equation 28 as a state equation using the stator current as a state variable:

$$\begin{bmatrix} \dot{i}_\alpha \\ \dot{i}_\beta \end{bmatrix} = \frac{1}{L_d} \begin{bmatrix} -R_s & -\omega_e\left(L_d - L_q\right) \\ \omega_e\left(L_d - L_q\right) & -R_s \end{bmatrix} \begin{bmatrix} i_\alpha \\ i_\beta \end{bmatrix} + \frac{1}{L_d} \begin{bmatrix} V_\alpha - e_\alpha \\ V_\beta - e_\beta \end{bmatrix} \tag{30}$$

Since the stator current is the only physical quantity that can be directly measured, the sliding surface is selected on the stator current path:

$$S(x) = \begin{bmatrix} \hat{i}_\alpha - i_\alpha \\ \hat{i}_\beta - i_\beta \end{bmatrix} = \begin{bmatrix} \tilde{i}_\alpha \\ \tilde{i}_\beta \end{bmatrix} \tag{31}$$

where

- $\hat{i}_\alpha$ and $\hat{i}_\beta$ are the estimated currents
- the superscript ^ indicates the estimated value
- the superscript "~" indicates the variable error which refers to the difference between the observed value and the actual measurement value

3.2.2.1.2 Design of ESMO for the IPMSM

Figure 3-16 shows the conventional PLL integrated into the SMO.

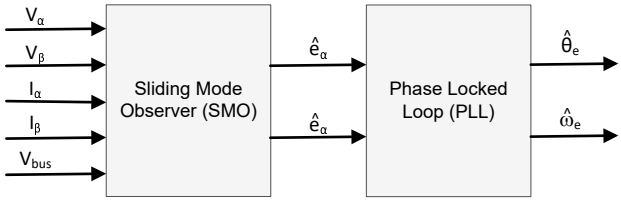

Figure 3-16. Block Diagram of eSMO With PLL for a PMSM

The traditional reduced-order sliding mode observer is constructed (Equation 32 shows the mathematical model) and Figure 3-17 shows the block diagram.

$$\begin{bmatrix} \dot{\hat{i}}_\alpha \\ \dot{\hat{i}}_\beta \end{bmatrix} = \frac{1}{L_d} \begin{bmatrix} -R_s & -\hat{\omega}_e\left(L_d - L_q\right) \\ \hat{\omega}_e\left(L_d - L_q\right) & -R_s \end{bmatrix} \begin{bmatrix} \hat{i}_\alpha \\ \hat{i}_\beta \end{bmatrix} + \frac{1}{L_d} \begin{bmatrix} V_\alpha - \hat{e}_\alpha + z_\alpha \\ V_\beta - \hat{e}_\beta + z_\beta \end{bmatrix} \tag{32}$$

where

- z_α and z_β are sliding mode feedback components and are defined in Equation 33

$$\begin{bmatrix} z_\alpha \\ z_\beta \end{bmatrix} = \begin{bmatrix} k_\alpha sign\left(\hat{i}_\alpha - i_\alpha\right) \\ k_\beta sign\left(\hat{i}_\beta - i_\beta\right) \end{bmatrix} \tag{33}$$

where

- k_α and k_β are the constant sliding mode gain designed by Lyapunov stability analysis

If k_α and k_β are positive and significant enough to provide the stable operation of the SMO, the k_α and k_β are large enough to hold $k_\alpha > max(|e_\alpha|)$ and $k_\beta > max(|e_\beta|)$.

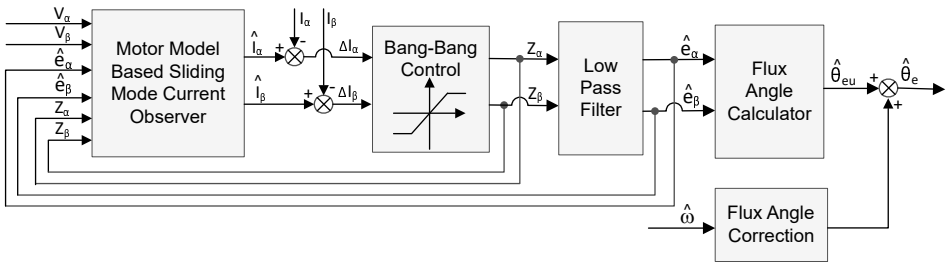

Figure 3-17. Block Diagram of Traditional Sliding Mode Observer

The estimated value of EEMF in α-β axes ($\hat{e}_\alpha$, $\hat{e}_\beta$) can be obtained with the low-pass filter from the discontinuous switching signals z_α and z_α:

$$\begin{bmatrix} \hat{e}_\alpha \\ \hat{e}_\beta \end{bmatrix} = \frac{\omega_c}{s + \omega_c} \begin{bmatrix} z_\alpha \\ z_\beta \end{bmatrix} \tag{34}$$

where

- $\omega_c = 2\pi f_c$ is the cutoff angular frequency of the LPF, which is typically selected according to the fundamental frequency of the stator current.

Therefore, the rotor position can be directly calculated from arc-tangent the back-EMF, defined in Equation 35:

$$\hat{\theta}_e = -\tan^{-1}\left(\frac{\hat{e}_\alpha}{\hat{e}_\beta}\right) \tag{35}$$

The low-pass filter removes the high-frequency term of the sliding mode function, which leads to phase delay. The delay can be compensated by the relationship between the cut-off frequency, ω_c and back-EMF frequency ω_e, which is defined as:

$$\Delta\theta_e = -\tan^{-1}\left(\frac{\omega_e}{\omega_c}\right) \tag{36}$$

Now the estimated rotor position is calculated by using the SMO method:

$$\hat{\theta}_e = -\tan^{-1}\left(\frac{\hat{e}_\alpha}{\hat{e}_\beta}\right) + \Delta\theta_e \tag{37}$$

In a digital control application, a time-discrete equation of the SMO is needed. The Euler method is the appropriate way to transform to a time-discrete observer. The time-discrete system matrix of Equation 32 in α-β coordinates is given by Equation 38 as:

$$\begin{bmatrix}\hat{i}_\alpha(n+1)\\ \hat{i}_\beta(n+1)\end{bmatrix}=\begin{bmatrix}F_\alpha\\ F_\beta\end{bmatrix}\begin{bmatrix}\hat{i}_\alpha(n)\\ \hat{i}_\beta(n)\end{bmatrix}+\begin{bmatrix}G_\alpha\\ G_\beta\end{bmatrix}\begin{bmatrix}V_\alpha^*(n)-\hat{e}_\alpha(n)+z_\alpha(n)\\ V_\beta^*(n)-\hat{e}_\beta(n)+z_\beta(n)\end{bmatrix} \quad (38)$$

where

- the matrix *[F]* and *[G]* are given by Equation 39 and Equation 40 as:

$$\begin{bmatrix}F_\alpha\\ F_\beta\end{bmatrix}=\begin{bmatrix}e^{-\frac{R_S}{L_d}}\\ e^{-\frac{R_S}{L_q}}\end{bmatrix} \quad (39)$$

$$\begin{bmatrix}G_\alpha\\ G_\beta\end{bmatrix}=\frac{1}{R_S}\begin{bmatrix}1-e^{-\frac{R_S}{L_d}}\\ 1-e^{-\frac{R_S}{L_q}}\end{bmatrix} \quad (40)$$

The time-discrete form of Equation 34 is given by Equation 41 as:

$$\begin{bmatrix}\hat{e}_\alpha(n+1)\\ \hat{e}_\beta(n+1)\end{bmatrix}=\begin{bmatrix}\hat{e}_\alpha(n)\\ \hat{e}_\beta(n)\end{bmatrix}+2\pi f_c\begin{bmatrix}z_\alpha(n)-\hat{e}_\alpha(n)\\ z_\beta(n)-\hat{e}_\beta(n)\end{bmatrix} \quad (41)$$

3.2.2.1.3 Rotor Position and Speed Estimation With PLL

With the arc tangent method, the accuracy of the position and velocity estimations are affected due to the existence of noise and harmonic components. To eliminate this issue, the PLL model can be used for velocity and position estimations in the sensorless control structure of the IPMSM. The PLL structure used with SMO is illustrated in Section 3.2.2.1.2. The back-EMF estimations $\hat{e}_\alpha$ and $\hat{e}_\beta$ can be used with a PLL model to estimate the motor angular velocity and position as shown in Figure 3-18.

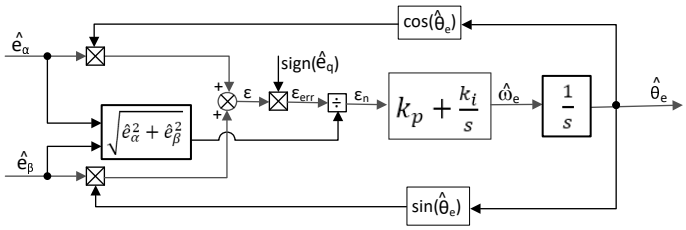

Figure 3-18. Block Diagram of Phase Locked Loop Position Tracker

Since $\hat{e}_\alpha = E\cos(\theta_e)$, $\hat{e}_\beta = E\sin(\theta_e)$ and $E = \omega_e\lambda_{pm}$, Equation 42 defines the position error.

$$\varepsilon=\hat{e}_\beta\cos(\hat{\theta}_e)-\hat{e}_\alpha\sin(\hat{\theta}_e)=E\sin(\theta_e)\cos(\hat{\theta}_e)-E\cos(\theta_e)\sin(\hat{\theta}_e)=E\sin(\theta_e-\hat{\theta}_e) \quad (42)$$

where

- E is the magnitude of the EEMF, which is proportional to the motor speed ω_e.

When $(\theta_e - \hat{\theta}_e) < \pi/2$, Equation 42 can be simplified as in Equation 43.

$$\varepsilon=E(\theta_e-\hat{\theta}_e) \quad (43)$$

Further, the position error after the normalization of the EEMF can be obtained:

$$\varepsilon_n=\theta_e-\hat{\theta}_e \quad (44)$$

According to the analysis, the simplified block diagram of the quadrature phase locked loop position tracker can be obtained as shown in Figure 3-19. The closed-loop transfer functions of the PLL can be expressed as:

$$\frac{\hat{\theta}_e}{\theta_e} = \frac{k_p s + k_i}{s^2 + k_p s + k_i} = \frac{2\xi\omega_n s + \omega_n^2}{s^2 + 2\xi\omega_n s + \omega_n^2} \quad (45)$$

where

- k_p is the proportional gain of the standard PI regulator
- k_i is the integral gain of the standard PI regulator
- ω_n is the natural frequency

The damping ratio, ξ, is given in Equation 46.

$$k_p = 2\xi\omega_n, \qquad k_i = \omega_n^2 \quad (46)$$

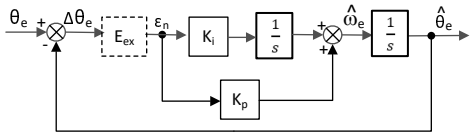

Figure 3-19. Simplified Block Diagram of Phase-Locked-Loop Position Tracker

3.2.3 Hardware Prerequisites for Motor Drive

The algorithm for controlling the motor makes use of sampled measurements of the motor conditions, including dc bus power supply voltage, the voltage on each motor phase, the current of each motor phase. There are a few hardware-dependent parameters that need to be set correctly to identify the motor properly and run the motor effectively using FOC. The following sections show how to calculate the current scale value, voltage scale value, and voltage filter pole for compressor and fan motors control with FAST or eSMO.

3.2.3.1 Current Sensing With Three-Shunt

The current through the motor is sampled by the microcontroller as part of the motor control algorithm during every PWM cycle. To measure bidirectional currents of the motor phase, that is, positive and negative currents, the circuits create a reference voltage of 1.65V. This offset reference voltage is created by a voltage follower with TLV9062. Figure 3-20 shows how the motor current is represented as a voltage signal, with filtering, amplification, and offset to the center of the ADC input range. This circuit is used for each phase of the three-phase motor. The transfer function of this circuit is given by Equation 47.

$$V_{OUT} = V_{OFFSET} + (I_{IN} \times R_{SHUNT} \times G_i) \quad (47)$$

where

- R_{SHUNT} = 0.02Ω
- V_{OFFSET} = 1.65V

The calculated resistance values lead to the sensing circuit shown in Figure 3-21, G_i is given by Equation 48.

$$G_i = \frac{R_{fb}}{R_{in}} = \frac{R20}{R18} = \frac{10.0K}{1.0K} = 10.0 \quad (48)$$

The maximum peak-to-peak current measurable by the microcontroller is given by Equation 49.

$$I_{scale\_max} = \frac{V_{ADC\_max}}{R_{SHUNT} \times G_i} = \frac{3.3}{0.02 \times 10} = 16.5A \quad (49)$$

The resulting 16.5A is the peak-to-peak value of ±8.25A. The following code snippet shows how this is defined for the compressor motor in the *user_mtr1.h* file:

```
//! \brief Defines the maximum current at the AD converter
#define USER_M1_ADC_FULL_SCALE_CURRENT_A         (16.5f)
```

Correct polarity of the current feedback is also important so that the microcontroller has an accurate current measurement. In this hardware board configuration, the negative pin of the shunt resistor, which is connected to ground, is also connected to the non-inverting pin of the operational amplifier. The highlighted sign is required to be configured to have correct polarity for the current feedback in software as shown in the following code snippet in motor1_drive.c:

```
// define the sign of current feedback based on hardware board
adcData[MTR_1].current_sf = -userParams[MTR_1].current_sf;
```

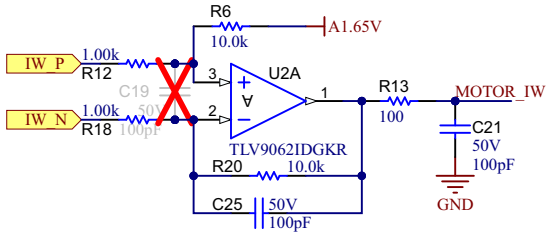

Figure 3-20. Motor Current Sensing Circuit With Three-Shunt

Implement the same calculation steps for a fan motor, and set the scale values in the *user_mtr2.h* file.

3.2.3.2 Motor Voltage Feedback

Voltage feedback is needed in the FAST estimator to allow the best performance at the widest speed range, the phase voltages are measured directly from the motor phases instead of a software estimate. The eSMO relies on software estimation values to represent the voltage phases without using the motor phase voltage sensing circuit. This software value (USER_ADC_FULL_SCALE_VOLTAGE_V) depends on the circuit that senses the voltage feedback from the motor phases. Figure 3-21 shows how the motor voltage is filtered and scaled for the ADC input range using a voltage feedback circuit based on resistor dividers. The similar circuit is used to measure both compressor and fan motors, and the DC bus.

The maximum phase voltage feedback measurable by the microcontroller in this reference design can be calculated as given in Equation 50, considering the maximum voltage for the ADC input is 3.3V.

$$V_{FS} = V_{ADC\_FS} \times G_v = 3.3V \times 137.07 = 452.32V \tag{50}$$

where

- G_V is attenuation factor which can be calculated from Equation 51

$$G_V = \frac{(R54 + R59 + R64 + R71)}{R71} = \frac{(332K + 332K + 332K + 7.32K)}{7.32K} = 137.07 \tag{51}$$

With that voltage feedback circuit, the following setting is made in user_mtr1.h:

```
//! \brief Defines the maximum voltage at the AD converter
#define USER_M1_ADC_FULL_SCALE_VOLTAGE_V         (452.32f)
```

The voltage filter pole is needed by the FAST estimator to allow an accurate detection of the voltage feedback. The filter needs to be low enough to filter out the PWM signals, and at the same time allow a high-speed voltage feedback signal to pass through the filter. As a general guideline, a cutoff frequency of a few hundred Hz is enough to filter out a PWM frequency of 5 to 20kHz. The hardware filter needs to only be changed when ultra-high-speed motors are run, which generate phase-voltage frequencies in the order of a few kHz.

Use Equation 52 to calculate the filter pole setting in this reference design.

$$f_{filter\_pole} = \frac{1}{(2 \times \pi \times R_{Parallel} \times C)} = 466.01 \quad Hz \tag{52}$$

$where,$
$C = 47nF$

$$R_{Parallel} = \left(\frac{(332K + 332K + 332K) \times 7.32K}{(332K + 332K + 332K) + 7.32K}\right) = 7.267k\Omega$$

The following code example shows how this is defined in user_mtr1.h:

```
//! \brief Defines the analog voltage filter pole location, Hz
#define USER_M1_VOLTAGE_FILTER_POLE_Hz           (466.01f)
```

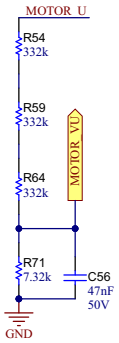

Figure 3-21. Motor Voltage Sensing Circuit

4 Hardware, Testing Requirements, and Test Results

4.1 Hardware Requirements

This section details the necessary equipment, test setup, and procedural instructions for the design board and software testing and validation.

4.1.1 Hardware Board Overview

Figure 4-1 shows an overview of a typical motor control with PFC running from AC power. The PFC stage enables wave shaping of the input AC current and provides the adjustable DC power for a three-phase motor.

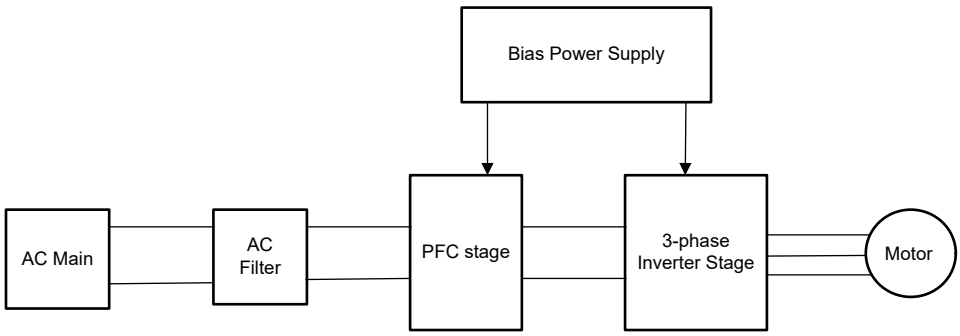

Figure 4-1. TIDA-010282 Hardware Board Block Diagram

The motor control board has functional groups that enable a complete motor drive system. The following is a list of the blocks on the board and the functions, Figure 4-2 shows the top view of the board and different blocks of the TIDA-010282 PCB.

- Power line input filter
- Digital totem pole PFC
  - Maximum power is up to 1.3kW
  - PFC with 75kHz switching frequency
  - Fast switching devices are GaN, and low switching devices are MOSFET
- Three-phase inverter
  - Up to 1.3kW, three-phase inverter supports PMSM or IPM
  - 15kHz switching frequency
  - Three shunts for current sensing
- Control
  - Support daughter board for TMS320F2800137 MCU in 48-pin LQFP package
  - 120MHz, 32-bit CPU with FPU and TMU
- Auxiliary power supply
  - Onboard +15V and +3.3V bias power supply

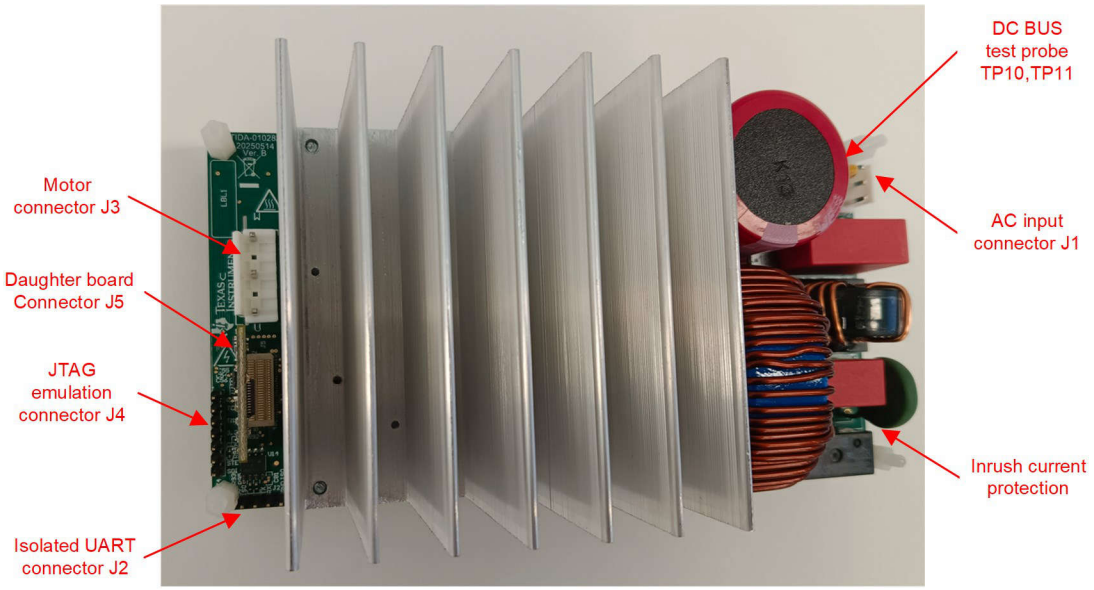

Figure 4-2. TIDA-010282 Reference Design Board Layout

TI recommends taking the following precautions when using the board:

- Do not touch any part of the board or components connected to the board when the board is energized.
- Use the AC Mains (wall power) supply to power the kit. TI recommends an isolation AC source.
- Do not touch any part of the board, the kit or the assembly when energized. (Though the power module heat sink is isolated from the board, high-voltage switching generates some capacitive coupled voltages over the heat sink body.)
- Control ground can be hot

4.1.2 Test Conditions

The following parameters and guidelines are recommended to test the reference design software:

- PFC Operation
  - For input, the power supply source must range from 85VAC to 265V AC. Set the input current limit of input AC source to 10A for full power test, but start with a lower current limit during initial board bring-up.
  - For output, use an electronic variable load or a variable resistive load, which must be rated for ≥ 400V and must vary the load current from 0mA to 5A.
- Motor Drive Operation
  - For input, the power supply source must range from 85V to 265V AC, if using the AC source. Set the input current limit of input AC source to 10A, but start with a lower current limit during initial board bring-up.
  - For output, use a three-phase PMSM with dynamo meters

4.1.3 Test Equipment Required for Board Validation

- Isolated AC source
- Digital oscilloscope
- Multimeter
- Electronic or resistive load
- DC power supply
- 1.3kW, three-phase PM synchronous motors
- Dynamo meters
- Three-phase power analyzer

4.2 Test Setup

Figure 4-2 shows the position of the blocks and the connectors on the board. Setup the hardware using the following steps:

1. Connect a JTAG emulator to connector J4 to debug or program the C2000 device.
   cJTAG mode with 2-pin (TMS and TCK) must be used for the external emulator.
2. Connect the motor wires to the terminals J3 after completing the first incremental build step.
3. Apply AC power supply or AC mains power to the inverter by connecting the power to J1.
   a. The maximum output of the DC power supply is 400VDC
   b. The maximum output of the AC power supply is 265VAC, 50Hz and 60Hz
   c. AC main power is 220VAC, 50Hz and 60Hz
4. Connect output terminals TP10 and TP11 to the electronic load maintaining correct polarity.
5. Connect multimeter, oscilloscope probes, and other measurement equipment to the probe or analyze various signals and parameters as desired. Only use appropriately rated equipment and follow proper isolation and safety practices.

Note

Add ferrite beads on JTAG signals and the USB cable if the external emulator has connectivity issues while testing. Make the connection lines as short as possible.

WARNING

The ground planes of both the power domains can be the same or different depending on hardware configuration. Meet proper isolation requirements before connecting any test equipment with the board to provide for the safety of yourself and the equipment. Review the GND connections before powering the board. An isolator is required if measurement equipment is connected to the board.

4.3 Test Results

The following sections show the test data from the design. The test results are divided in multiple sections that cover the steady state performance and data, functional performance waveforms, and transient performance waveforms of the fan and compressor motor.

4.3.1 Functional Waveforms

Figure 4-3 is a screen shot of 15V and 3.3V bias supply when powered onboard. The following displays shows 3.3V is set up when the 15V voltage rail reaches 12.7V.

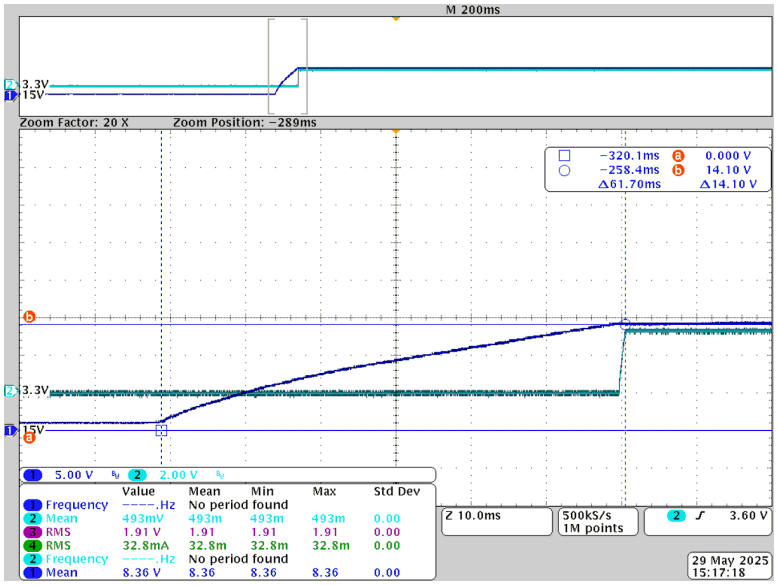

CH1 (Blue): 15VDC

CH2 (Dark Green): 3.3VDC

Figure 4-3. 15V and 3.3V Powering On

Figure 4-3 is a screen shot 15V and 3.3V bias supply when the board is powered off. Since the 5V DC/DC TPS562206 has 12.7VDC enable voltage, and has 1.9V hysteresis voltage, this prevents any bounce up after 3.3V falls down to zero.

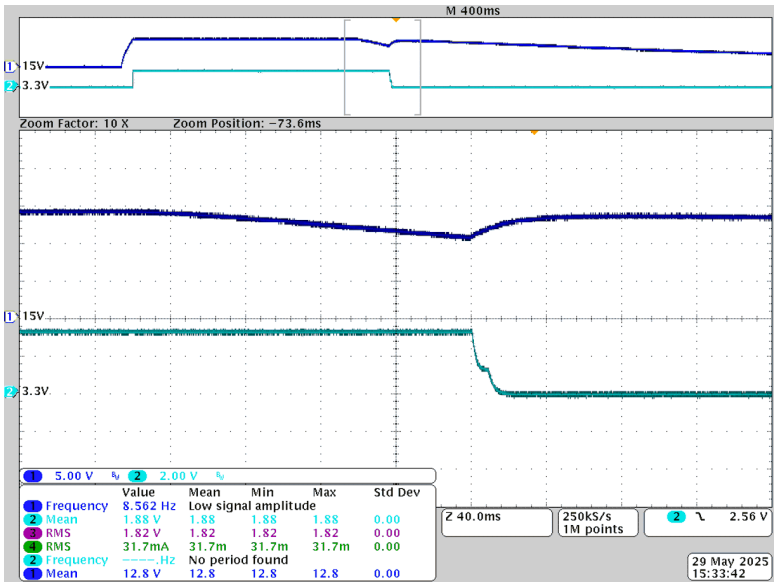

CH1 (Blue): 15VDC

CH2 (Dark Green): 3.3VDC

Figure 4-4. 15V and 3.3V Powering Off

GaN devices exhibit extremely fast slew rates, permitting remarkably short dead times in high-performance power electronic applications. Figure 4-5 displays a 300ns dead time for PFC circuit using Gallium Nitride (GaN) transistors.

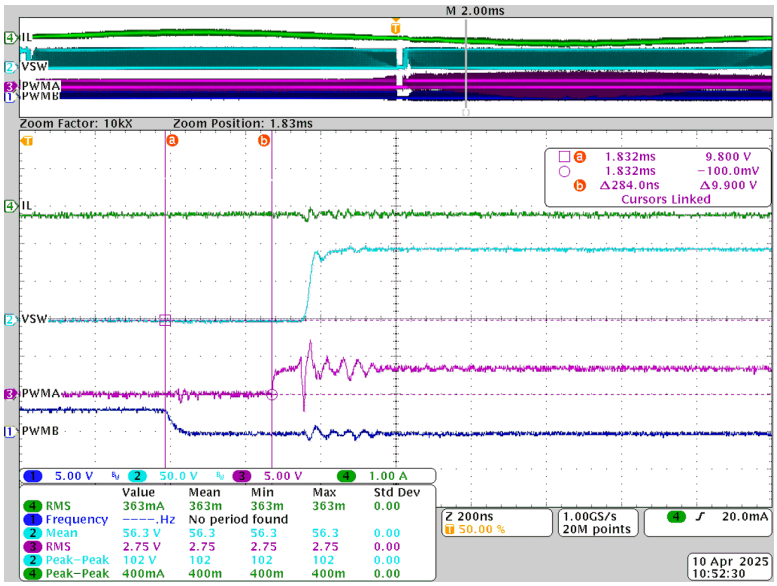

CH1 (Blue): PWM for Bottom GaN
CH2 (Light Blue): Switching Node Voltage
CH3 (Purple): PWM for Top GaN
CH4 (Green): Boost Inductor current

Figure 4-5. 300ns PFC Dead Time for GaN

Figure 4-6 is a screen shot of 100ns dead time for motor inverter stage.

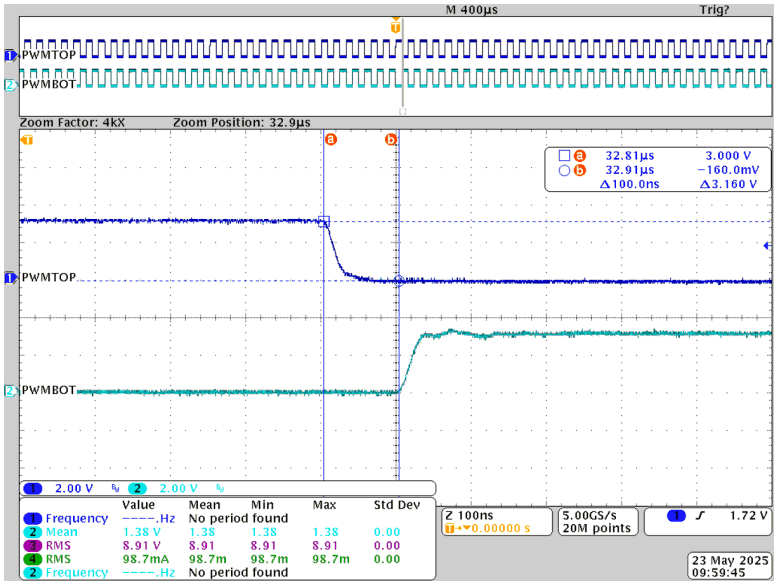

CH1 (Blue): PWM for Top side GaN
CH2 (Light Blue): PWM for bottom side GaN

Figure 4-6. 100ns Dead Time for Motor Inverter

Figure 4-7 is a screen shot of $2A_{RMS}$ motor phase current.

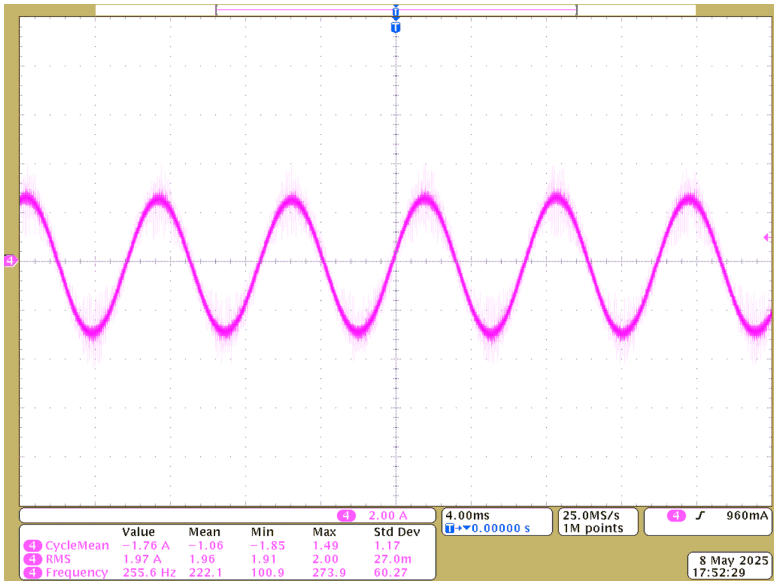

CH4 (Pink): Measured motor phase current with a current probe

Figure 4-7. Motor Phase Current

5 Design and Documentation Support

5.1 Design Files

5.1.1 Schematics

To download the schematics, see the design files at TIDA-010282.

5.1.2 Bill of Materials

To download the bill of materials (BOM), see the design files at TIDA-010282.

5.1.3 Altium Project

To download the Altium project files, see the design files at TIDA-010282.

5.1.4 Gerber Files

To download the Gerber files, see the design files at TIDA-010282.

5.1.5 PCB Layout Recommendations

This reference design is implemented using a PCB with two layer, 1oz copper with a single-side SMD component placement considering the cost sensitivity of the application. There are several important aspects to remember while designing the PCB. In the following list, system-level placement and layout of each block is explained.

Components in the high-power path are kept on the outer edges of the PCB using the minimum distance possible. The microcontroller is placed at the center considering the optimum distance from all the power blocks that need to be controlled. Pin assignment is set to minimize the control signal trace and feedback signal trace distance and the crossing between analog and digital signals.

- AC Line Protection and EMI Filter
  - AC line protection components are closely placed within the minimum distance of the connection path. Earth connection guarding is provided around the protection and EMI filter circuit.
  - An active EMI filter is placed at the optimum distance so as to stay closer to switching and to have the minimum distance to connect to the EARTH terminal.
- IPFC Drive

  In IPFC drive, three current paths are very critical for PCB layout - the high power AC loop, DC loop, and gate drive loop. These paths need to be short with the maximum width possible to reduce parasitic-loop inductance.

  - AC loop – Consists of diode bridge (source), inductor, and MOSFET drain and MOSFET source (return). On this loop, especially the connection between the inductor, the MOSFET Drain and Diode Anode handle high frequency and high power. Special care is taken while connecting this node to minimize parasitic inductance by reducing the distance and increasing the copper area.
  - DC loop – Consists of diode bridge (source), inductor, diode, capacitor, load (return). To distribute the RMS current stress evenly, place the bank of electrolyte capacitors such that the electrical distance of each one from the diode cathodes remains approximately the same. This design uses a copper plane for the V_{DC} and PGND connection. To suppress the high-frequency component, a metal-film capacitor is placed just next to the cathode of the diode. The capacitor minimizes the loop inductance significantly.
  - Gate drive loop – Consists of driver power supply (source), gate driver IC, MOSFET gate, and MOSFET source pin (return). This design uses parallel arrangement for two phases of IPFC to minimize the other two AC/DC loops. Because of this parallel arrangement, the outer phase MOSFET gate is inaccessible to the gate driver. An SMD insulated thick jumper is used to connect the gate driver signal to MOSFET gate.
- Compressor and Fan Drive
  - With the highest ripple requirement, a compressor drive is placed closest to the DC bus capacitor bank of the IPFC drive and a fan is placed next to the compressor.
  - The low-side shunt resistor method with 4-wire sensing is implemented for current sensing. A differential pair with impedance matching resistors is used to connect the sensing signal from the shunt resistors to the op-amp circuit. Shunt resistors are placed near the module with an immediate ground copper plane connection.

- Auxiliary Power Supply
  - With the lowest power and ripple requirement, auxiliary power is placed after the fan drive. A dedicated copper plane is used to connect the APS ground to the DC bus capacitor bank. This arrangement minimizes interference between the high frequency and high power motor current and control circuit.

5.2 Tools

CCSTUDIO	Code Composer Studio™ integrated development environment (IDE) for TI's microcontrollers and processors. Code Composer Studio is comprised of a rich suite of tools used to build, debug, analyze, and optimize embedded applications. Code Composer Studio is available across Microsoft® Windows®, Linux®, and macOS® platforms.
C2000WARE-MOTORCONTROL-SDK	MotorControl software development kit (SDK) for C2000™ MCUs. MotorControl SDK for C2000™ microcontrollers (MCU) is a cohesive set of software infrastructure, tools, and documentation designed to minimize C2000 real-time controller based motor control system development time targeted for various three-phase motor control applications.

5.3 Documentation Support

1. Texas Instruments, *TMS320F28002x Real-Time Microcontrollers Data Sheet*
2. Texas Instruments, *TMS320F28002x Real-Time Microcontrollers Technical Reference Manual*
3. Texas Instruments, *TMS320F28003x Microcontrollers Data Sheet*
4. Texas Instruments, *TMS320F28003x Real-Time Microcontrollers Technical Reference Manual*
5. Texas Instruments, *TMS320F280013x Microcontrollers Data Sheet*
6. Texas Instruments, *TMS320F280013x Real-Time Microcontrollers Technical Reference Manual*
7. Texas Instruments, *InstaSPIN-FOC and InstaSPIN-MOTION User's Guide*
8. Texas Instruments, *Motor Control SDK Universal Project and Lab User's Guide*
9. Texas Instruments, *C2000™ Software Frequency Response Analyzer (SFRA) Library and Compensation Designer User's Guide*
10. Texas Instruments, *Two-Phase Interleaved PFC Converter w/ Power Metering Test Results Design Guide*
11. Texas Instruments, *Sensorless-FOC for PMSM With Single DC-Link Shunt Application Note*
12. Texas Instruments, *TIDM-1022 Valley Switching Boost Power Factor Correction (PFC) Reference Design*
13. Texas Instruments, *C2000 SysConfig Application Note*

5.4 Support Resources

TI E2E™ support forums are an engineer's go-to source for fast, verified answers and design help — straight from the experts. Search existing answers or ask your own question to get the quick design help you need.

Linked content is provided "AS IS" by the respective contributors. They do not constitute TI specifications and do not necessarily reflect TI's views; see TI's Terms of Use.

5.5 Trademarks

C2000™ and TI E2E™ are trademarks of Texas Instruments.
Microsoft® and Windows® are registered trademarks of Microsoft Corporation.
Linux® is a registered trademark of Linus Torvalds.
macOS® is a registered trademark of Apple Inc.
All trademarks are the property of their respective owners.

6 About the Author

HELY ZHANG is a System Application Engineer at Texas Instruments, where he is responsible for developing home appliance related power delivery and motor inverters. Hely earned his masters degree from Anhui University of Science and Technology with Power electronics in 2002, and worked in SolarEdge and General Electric before joining TI.

IMPORTANT NOTICE AND DISCLAIMER

TI PROVIDES TECHNICAL AND RELIABILITY DATA (INCLUDING DATA SHEETS), DESIGN RESOURCES (INCLUDING REFERENCE DESIGNS), APPLICATION OR OTHER DESIGN ADVICE, WEB TOOLS, SAFETY INFORMATION, AND OTHER RESOURCES “AS IS” AND WITH ALL FAULTS, AND DISCLAIMS ALL WARRANTIES, EXPRESS AND IMPLIED, INCLUDING WITHOUT LIMITATION ANY IMPLIED WARRANTIES OF MERCHANTABILITY, FITNESS FOR A PARTICULAR PURPOSE OR NON-INFRINGEMENT OF THIRD PARTY INTELLECTUAL PROPERTY RIGHTS.

These resources are intended for skilled developers designing with TI products. You are solely responsible for (1) selecting the appropriate TI products for your application, (2) designing, validating and testing your application, and (3) ensuring your application meets applicable standards, and any other safety, security, regulatory or other requirements.

These resources are subject to change without notice. TI grants you permission to use these resources only for development of an application that uses the TI products described in the resource. Other reproduction and display of these resources is prohibited. No license is granted to any other TI intellectual property right or to any third party intellectual property right. TI disclaims responsibility for, and you will fully indemnify TI and its representatives against, any claims, damages, costs, losses, and liabilities arising out of your use of these resources.

TI’s products are provided subject to TI’s Terms of Sale or other applicable terms available either on ti.com or provided in conjunction with such TI products. TI’s provision of these resources does not expand or otherwise alter TI’s applicable warranties or warranty disclaimers for TI products.

TI objects to and rejects any additional or different terms you may have proposed.

Mailing Address: Texas Instruments, Post Office Box 655303, Dallas, Texas 75265